Title: Auxin-sensitive Aux/IAA proteins mediate drought tolerance in Arabidopsis by regulating glucosinolate levels

Authors: M. Salehin[1], B. Li[2], M. Tang[2], E. Katz[2], L. Song[3], J. R. Ecker[3], D. Kliebenstein[2], and M. Estelle[1*]

Affiliations:

[1]Section of Cell and Developmental Biology and Howard Hughes Medical Institute, University of California San Diego, La Jolla CA., 92093.

[2] Department of Plant Sciences, University of California Davis, Davis CA 95616.

[3] Genomic Analysis Laboratory, Howard Hughes Medical Institute and The Salk Institute for Biological Studies, La Jolla, CA 92037

*Correspondence to: mestelle@ucsd.edu

Abstract: A detailed understanding of abiotic stress tolerance in plants is essential to provide food security in the face of increasingly harsh climatic conditions. Glucosinolates (GLSs) are secondary metabolites found in the Brassicaceae that protect plants from herbivory and pathogen attack. Here we report that in Arabidopsis, aliphatic GLS levels are regulated by the auxin-sensitive Aux/IAA repressors IAA5, IAA6, and IAA19. These proteins act in a transcriptional cascade that maintains expression of GLS levels when plants are exposed to drought conditions. Loss of IAA5/6/19 results in reduced GLS levels and decreased drought tolerance. Further, we show that this phenotype is associated with a defect in stomatal regulation. Application of GLS to the *iaa5,6,19* mutants restores stomatal regulation and normal drought tolerance. GLS action is dependent on the receptor kinase GHR1, suggesting that GLS may signal via reactive oxygen species. These results provide a novel connection between auxin signaling, GLS levels and drought response.

One Sentence Summary: Aux/IAA proteins promote drought tolerance by regulating glucosinolate levels.

Main Text: The Aux/IAA transcriptional repressors have a central role in auxin signaling. In the presence of auxin, the Aux/IAAs are degraded through the action of the ubiquitin E3-ligase $SCF^{TIR1/AFB}$, resulting in de-repression of transcription by the AUXIN RESPONSE FACTOR (ARF) transcription factors(*1, 2*). Although the mechanisms of auxin perception and Aux/IAA degradation are well known, other aspects of Aux/IAA regulation remain poorly understood. In particular, the factors that regulate transcription of the *Aux/IAA* genes are mostly unknown. Recently, we showed that three *Aux/IAA* genes, *IAA5, IAA6,* and *IAA19* are directly regulated by the DREB2A and DREB2B transcription factors and that recessive mutations in these *IAA* genes result in a decrease in drought tolerance (*3*).

To determine the molecular basis of the loss of drought tolerance in *iaa5, iaa6,* and *iaa19* mutant plants, we used RNAseq to identify genes that were differentially regulated in Col-0 vs. the *iaa5 iaa6 iaa19* (*iaa5,6,19*) triple mutant when exposed to desiccation stress (Table S1). A total of 651 genes were differentially expressed between the mutant and Col-0 under these conditions (FDR < 0.001), 439 down-regulated and 212 up-regulated. A gene ontology search revealed that 12 genes that function in the aliphatic glucosinolate (GLS) biosynthetic pathway are down-regulated in *iaa5,6,19* (Fig. 1A, B). In contrast, expression of these genes is not significantly affected by dehydration stress in Col-0. We confirmed these results by quantitative RT-PCR (qRT-PCR) (Fig. S1A).

Because the aliphatic GLS biosynthetic enzymes are down-regulated in *iaa5,6,19* mutants during drought stress, we wondered if the levels of GLSs were also affected. To test this, we measured GLS levels in stress treated Col-0 and *iaa5,6,19* mutants at time intervals. Indolic GLSs were unaltered (Table S2). However, the level of 4-methylsulfinyl glucosinolate (4-MSO), the most abundant aliphatic glucosinolate in Arabidopsis (Col-0), was sharply decreased in *iaa5, 6, 19* plants after 1 hr and 3 hr of desiccation (Fig. 1C). This data shows that down-regulation of aliphatic GLS biosynthetic enzymes in *iaa5, 6, 19* mutants results in decreased GLS levels.

GLSs are well known for their role in plant defense and innate immunity, although recent studies also suggest that they may have a role in regulating plant growth (*4-8*). These secondary metabolites are found primarily in the Brassicaceae, a family that includes many economically important crops (*6*). GLSs are broken down by the enzyme myrosinase into isothiocyanates and related compounds, which are toxic to insect herbivores and other plant pathogens (*7-10*). To determine if decreased drought tolerance in the *iaa5,6,19* mutant is related to reduced GLS levels, we measured the effects of mutations in GLS biosynthetic genes on response to drought. We employed two assays; growth of seedlings on agar medium containing PEG, and growth of plants in pots after withholding water. We first characterized mutants in the *CYP79F1* and *CYP79F2* genes, encoding enzymes that convert elongated methionine to aldoximes (Fig. 1A). Both mutants, as well as the double mutant, are less tolerant to both PEG treatment and water withholding (Fig. 2A, B; Fig. S2B, C). Similarly, loss of CYP83A1, responsible for conversion of aldoximes to *aci*-Nitro compounds, results in reduced tolerance to water withholding in pots (Fig. S2D). These results indicate that loss of aliphatic GLS compounds results in decreased drought tolerance, providing an explanation for the phenotype of the *iaa5,6,19* mutant.

The MYB28 and MYB29 transcription factors are known to regulate genes in the aliphatic GLS biosynthetic pathway, including the *CYP79F1/F2* and *CYP83A1* genes (*11-14*). Indeed, aliphatic GLS levels in the *myb28 myb29* double mutant are extremely low, whereas over-expression of either *MYB28* or *MYB29* results in elevated aliphatic GLS levels (*12-15*). Thus, it is possible that the effects of the *iaa5,6,19* mutations on the pathway are mediated by changes in expression of these transcription factor genes. Examination of our RNAseq data revealed that *MYB28* is down-regulated in the triple mutant in response to stress. *MYB29* is expressed at a very low level in seedlings. We confirmed this by qRT-PCR (Fig. S1). When we determined the response of the *myb28 mby29* double mutant to water withholding we found that it is less tolerant than the wild type, further support for the idea and GLSs are required for drought tolerance (Fig. 2C; Fig. S3A). Since overexpression of *MYB28* and *MYB29* increases GLS levels, we also tested the behavior of these lines in our assays. Strikingly, we found that both lines displayed strongly increased drought tolerance (Fig. 2D, Fig. S3B) further confirming that GLSs confer drought tolerance. We also tested the effect of over-expression of the *AOP2* gene on drought tolerance. Over-expression of this gene in Col-0 results in an increase in aliphatic GLS levels, although less than in lines over-expressing *MYB28 (16)*. The results in Fig 2D and Fig. S3B show that increased AOP2 levels results in a modest but statistically significant increase in drought tolerance.

If decreased drought tolerance in *iaa5,6,19* plants is due to a GLS deficiency then over-expression of *MYB28* or *MYB29* in the triple mutant may ameliorate the effects of the mutations. Indeed, when we cross the *35S:MYB28* or *35S:MYB29* transgene into the *iaa19-1* mutant the result is the restoration of wild-type levels of drought tolerance to the mutant line (Figure 2E).

Although IAA5, 6, and 19 are required for expression of *MYB28,* they are unlikely to directly regulate *MYB28* because they are transcriptional repressors (*1*). To identify transcription factors that might be direct targets of the Aux/IAAs, and that might regulate *MYB28* expression, we searched our RNAseq data for factors that are up-regulated in the triple mutant in response to stress. One interesting candidate was *WRKY63*, also known as *ABA OVERLY SENSITIVE3* (*abo3*)(*17*). The *abo3* mutant was originally isolated because it is hypersensitive to ABA in seedlings. Our qRT-PCR experiments confirmed that *WRKY63* is up-regulated in response to dehydration in the triple mutant compared to the wild type (Fig. 3A). Examination of the promoter region of the *WRKY63* gene revealed the presence of two tandemly repeated *AuxRE* elements (-350 to -361), known to bind ARF transcription factors (*2*). To determine if IAA19 binds to these sequences, we performed a ChIP-PCR analysis using a *rAA19-YPet-His-FLAG* line. The results, shown in Fig 3B, show that recovery of *AuxRE* sequences is significantly enriched in the IP from *rIAA19-YPet-His-FLAG* compared to the control indicating that IAA19 binds to this sequence, presumably indirectly through an interaction with an ARF transcription factor.

To determine if WRKY63 might regulate *MYB28/29* expression, we measured RNA levels in two *35S:WRKY63* lines by qRT-PCR and found that expression of both genes was reduced suggesting that WRKY63 acts to repress expression of the *MYB* genes (Fig 3C) (*18*). Finally, we measured drought tolerance of the *35S:WRKY63* lines as well as the knockout mutant *wrky63-1*. As shown in Fig. 3D and Fig. S3B, the mutant has a normal response to water withholding. However, both over-expression lines are less drought tolerant consistent with reduced expression of *MYB28/29*. We note that *WRKY63* is a member of small clade of 4 genes. It is possible that these genes have an overlapping function in regulation of *MYB28/29.* We note that our analysis of WRKY63 differs from the earlier work showing that the *abo1* mutant is less drought tolerance *(17*). The reason for this discrepancy is unclear.

In considering how aliphatic GLSs may regulate drought response, we noted that these compounds have been reported to promote stomatal closure. In addition, the myrosinase TGG1 is one of the most abundant proteins in Arabidopsis guard cells suggesting that GLS compounds may have an important role in guard cell function (*19*). Further, isothiocyanate, a GLS metabolite, closes stomata in Arabidopsis (*20, 21*). To determine if a defect in stomatal regulation might be responsible for reduced drought tolerance in the *iaa5,6,19* and *myb28 myb29* lines, we first examined the stomatal response to drought in epidermal peels. As expected, the stomata on Col-0 plants close in response to drought conditions (Fig. 4A). In contrast, the stomata on both mutant lines failed to respond. We next asked whether application of 4-MSO would promote stomatal closure in wild-type and mutant plants. As a control we also applied abscisic acid (ABA) The results shown in Fig. 4B demonstrate that all three genotypes respond to both ABA and 4-MSO. We further tested the effects of 4-MSO on light-induced opening of stomata from dark-adapted plants. The results in Fig 4C show that 4-MSO inhibits this response in Col-0 and *iaa5,6,19* plants. These results suggest that the primary basis for reduced drought tolerance in the *iaa5,6,19* line is failure to close stomata in drought conditions. To test this possibility, we applied 4-MSO to wild-type and mutant plants subjected to water withholding in pots. The results in Fig. 4D and Fig. S2A show that application of this GLS restores drought tolerance in the mutant to wild-type levels.

To determine if all GLS compounds promote stomatal closure, we applied indol-3-ylmethylglucosinolate (I3M), an indolic GLS that is abundant in Arabidopsis, to Col-0. The results in Fig. 4C demonstrate that I3M is unable to inhibit light-induced stomatal opening in either Col-0 or the triple mutant, indicating that not all glucosinolates have the same efficacy. Similar results were obtained in an experiment where we tested the ability of I3M to promote stomatal closure in light grown plants (Fig 4E). We also tested a second aliphatic GLS, sinigrin hydrate (SH) that is abundant in many Arabidopsis ecotypes, although not Col-0 (*22*). Like 4-MSO, SH promoted closure in Col-0 and in the *abi1-1* mutant (Fig S3C). Thus, it is possible that this activity is restricted to aliphatic GLS compounds, although additional studies are required to explore this possibility further.

ABA is known to play a key role in stomatal regulation (*23*). We investigated potential interactions between GLS and ABA by testing the response of *iaa5,6,19* to ABA treatment. The results in Fig. 4B show that the mutant line does respond to ABA, indicating that GLS is not required for the ABA response. Further, we found that the *abi1* mutant, which is deficient in ABA regulation of stomatal closure, has a normal response to GLS (Fig. 4F) (*23*). These results suggest that GLS and ABA can act independently to regulate stomata. This is consistent with a recent study showing that GLS and ABA have an additive effect on stomatal closure (*24*).

Reactive oxygen species (ROS) play an important role in stomatal regulation. One of the effects of ABA is to stimulate production of extracellular ROS through the RESPIRATORY BURST OXIDASE HOMOLOG D (RBOHD)(*23*). Extracellular ROS than acts through the receptor kinase GUARD CELL HYDROGEN PEROXIDE-RESISTANT 1 (GHR1) to regulate the SLOW ANION ACTIVATING CHANNEL 1(*23*). Since isothiocyanates (ITC), products of GLS metabolism, are known to promote stomatal closure via ROS, we wondered if GHR1 is required for response to GLS(*21*). The results in Fig. 4G show that the *grh1* mutant is resistant to the effects of 4-MSO on stomata indicating that GLS likely acts through production of ROS.

Since loss of the auxin-sensitive repressors IAA5, IAA6, and IAA19 in the *iaa5,6,*19 results in decreased expression of GLS biosynthetic genes, we predict that the reduction in the levels of these proteins after auxin treatment would have the same effect. Indeed, treatment of seedlings with 10 μM IAA for 2 hours results in reduced expression of the GLS genes (Fig. S3D). Further, we predict that mutations which stabilize the Aux/IAA proteins will increase both GLS levels and drought tolerance. The TIR1/AFB family of auxin co-receptors consists of 6 members in Arabidopsis that act in an overlapping fashion to regulate auxin-dependent transcription throughout the plant. To determine the role of the TIR1/AFBs in GLS regulation we measured GLS levels in two higher order *tir1/afb* lines, *afb1,3,4,5* and *afb2,3,4,5* (*25*). Both lines had significantly higher GLS levels than either Col-0 or *iaa5,6,19* in 7-day-old seedlings (Fig. 4H). After one hour of desiccation, GLS levels dropped in all three mutant genotypes. In the case of the *iaa5,6,19* line, GLS levels were much lower than Col-0, while in *afb1,3,4,5* and *afb2,3,4,5*, levels were similar to Col-0. We also determined the effects of water withholding on these genotypes. The results in Fig 4I and Fig. S3E show that both *afb* lines are significantly more drought tolerant than Col-0.

The major plant hormones are all secondary metabolites with ancient signaling functions. Here we show that GLSs also act as chemical signals that regulate stomatal aperture during drought stress. Desiccation results in a rapid decrease in auxin response in seedlings, an effect that probably results in decreased growth*(3)*. By utilizing auxin to regulate stomatal aperture, the plant may integrate growth and stomatal regulation in drought conditions.

References and Notes

1.M. Salehin, R. Bagchi, M. Estelle, SCFTIR1/AFB-Based Auxin Perception: Mechanism and Role in Plant Growth and Development. *Plant Cell* **27**, 9-19 (2015).
2.D. Weijers, D. Wagner, Transcriptional Responses to the Auxin Hormone. *Annual review of plant biology* **67**, 539 (2016).
3.E. Shani *et al.*, Plant stress tolerance requires auxin-sensitive Aux/IAA transcriptional repressors. Current Biology. *Current Biology* **27**, 437-444 (2017).

4.E. Katz *et al.*, The glucosinolate breakdown product indole-3-carbinol acts as an auxin antagonist in roots of Arabidopsis thaliana. *Plant J* **82**, 547-555 (2015).
5.F. G. Malinovsky *et al.*, An evolutionarily young defense metabolite influences the root growth of plants via the ancient TOR signaling pathway. *Elife* **6**, (2017).
6.B. A. Halkier, J. Gershenzon, Biology and biochemistry of glucosinolates. *Annu Rev Plant Biol* **57**, 303-333 (2006).
7.P. Bednarek *et al.*, A glucosinolate metabolism pathway in living plant cells mediates broad-spectrum antifungal defense. *Science* **323**, 101-106 (2009).
8.N. K. Clay, A. M. Adio, C. Denoux, G. Jander, F. M. Ausubel, Glucosinolate metabolites required for an Arabidopsis innate immune response. *Science* **323**, 95-101 (2009).
9.U. Wittstock, J. Gershenzon, Constitutive plant toxins and their role in defense against herbivores and pathogens. *Curr Opin Plant Biol* **5**, 300-307 (2002).
10.J. Fan *et al.*, Pseudomonas sax genes overcome aliphatic isothiocyanate-mediated non-host resistance in Arabidopsis. *Science* **331**, 1185-1188 (2011).
11.T. Gigolashvili, M. Engqvist, R. Yatusevich, C. Müller, U. I. Flügge, HAG2/MYB76 and HAG3/MYB29 exert a specific and coordinated control on the regulation of aliphatic glucosinolate biosynthesis in Arabidopsis thaliana. *New Phytol* **177**, 627-642 (2008).
12.T. Gigolashvili, R. Yatusevich, B. Berger, C. Müller, U. I. Flügge, The R2R3-MYB transcription factor HAG1/MYB28 is a regulator of methionine-derived glucosinolate biosynthesis in Arabidopsis thaliana. *Plant J* **51**, 247-261 (2007).
13.I. E. Sonderby, M. Burow, H. C. Rowe, D. J. Kliebenstein, B. A. Halkier, A complex interplay of three R2R3 MYB transcription factors determines the profile of aliphatic glucosinolates in Arabidopsis. *Plant Physiol* **153**, 348-363 (2010).
14.M. Y. Hirai *et al.*, Omics-based identification of Arabidopsis Myb transcription factors regulating aliphatic glucosinolate biosynthesis. *Proc Natl Acad Sci U S A* **104**, 6478-6483 (2007).
15.I. E. Sønderby *et al.*, A systems biology approach identifies a R2R3 MYB gene subfamily with distinct and overlapping functions in regulation of aliphatic glucosinolates. *PLoS One* **2**, e1322 (2007).
16.A. M. Wentzell *et al.*, Linking metabolic QTLs with network and cis-eQTLs controlling biosynthetic pathways. *PLoS Genet* **3**, 1687-1701 (2007).
17.X. Ren *et al.*, ABO3, a WRKY transcription factor, mediates plant responses to abscisic acid and drought tolerance in Arabidopsis. *Plant J* **63**, 417-429 (2010).
18.O. Van Aken, B. Zhang, S. Law, R. Narsai, J. Whelan, AtWRKY40 and AtWRKY63 modulate the expression of stress-responsive nuclear genes encoding mitochondrial and chloroplast proteins. *Plant Physiol* **162**, 254-271 (2013).
19.Z. Zhao, W. Zhang, B. A. Stanley, S. M. Assmann, Functional proteomics of Arabidopsis thaliana guard cells uncovers new stomatal signaling pathways. *Plant Cell* **20**, 3210-3226 (2008).
20.M. S. Hossain *et al.*, Glucosinolate degradation products, isothiocyanates, nitriles, and thiocyanates, induce stomatal closure accompanied by peroxidase-mediated reactive oxygen species production in Arabidopsis thaliana. *Biosci Biotechnol Biochem* **77**, 977-983 (2013).
21.M. A. Khokon *et al.*, Allyl isothiocyanate (AITC) induces stomatal closure in Arabidopsis. *Plant Cell Environ* **34**, 1900-1906 (2011).
22.M. Francisco *et al.*, The Defense Metabolite, Allyl Glucosinolate, Modulates Arabidopsis thaliana Biomass Dependent upon the Endogenous Glucosinolate Pathway. *Front Plant Sci* **7**, 774 (2016).
23.S. Munemasa *et al.*, Mechanisms of abscisic acid-mediated control of stomatal aperture. *Curr Opin Plant Biol* **28**, 154-162 (2015).
24.M. Zhu, S. M. Assmann, Metabolic Signatures in Response to Abscisic Acid (ABA) Treatment in Brassica napus Guard Cells Revealed by Metabolomics. *Sci Rep* **7**, 12875 (2017).
25.M. J. Prigge, N. Kadakia, K. Greenham, M. Estelle. (bioRxiv, 2019).
26.I. E. Sønderby *et al.*, A systems biology approach identifies a R2R3 MYB gene subfamily with distinct and overlapping functions in regulation of aliphatic glucosinolates. *PLoS One* **2**, e1322 (2007).

27.O. Van Aken, B. Zhang, S. Law, R. Narsai, J. Whelan, AtWRKY40 and AtWRKY63 modulate the expression of stress-responsive nuclear genes encoding mitochondrial and chloroplast proteins. *Plant Physiol* **162**, 254-271 (2013).
28.J. Leung *et al.*, Arabidopsis ABA response gene ABI1: features of a calcium-modulated protein phosphatase. *Science* **264**, 1448-1452 (1994).
29.D. Hua *et al.*, A plasma membrane receptor kinase, GHR1, mediates abscisic acid- and hydrogen peroxide-regulated stomatal movement in Arabidopsis. *Plant Cell* **24**, 2546-2561 (2012).
30.J. M. Alonso, A. N. Stepanova, A recombineering-based gene tagging system for Arabidopsis. *Methods Mol Biol* **1227**, 233-243 (2015).
31.S. J. Clough, A. F. Bent, Floral dip: a simplified method for Agrobacterium-mediated transformation of Arabidopsis thaliana. *Plant J* **16**, 735-743 (1998).
32.M. I. Love, W. Huber, S. Anders, Moderated estimation of fold change and dispersion for RNA-seq data with DESeq2. *Genome Biol* **15**, 550 (2014).
33.H. Mi *et al.*, PANTHER version 11: expanded annotation data from Gene Ontology and Reactome pathways, and data analysis tool enhancements. *Nucleic Acids Res* **45**, D183-D189 (2017).
34.M. Ashburner *et al.*, Gene ontology: tool for the unification of biology. The Gene Ontology Consortium. *Nat Genet* **25**, 25-29 (2000).
35.The Gene Ontology Consortium, Expansion of the Gene Ontology knowledgebase and resources. *Nucleic Acids Res* **45**, D331-D338 (2017).
36.T. D. Schmittgen, K. J. Livak, Analyzing real-time PCR data by the comparative C(T) method. *Nat Protoc* **3**, 1101-1108 (2008).
37.E. J. Chapman *et al.*, Hypocotyl transcriptome reveals auxin regulation of growth-promoting genes through GA-dependent and -independent pathways. *PLoS One* **7**, e36210 (2012).
38.D. J. Kliebenstein *et al.*, Genetic control of natural variation in Arabidopsis glucosinolate accumulation. *Plant Physiol* **126**, 811-825 (2001).
39.L. S. Bates, R. P. Waldren, I. D. Teare, Rapid Determination of free proline for water-stress studies. *Plant Soil* **39**, 205-207 (1973).
40.G. B. Bhaskara, T. H. Yang, P. E. Verslues, Dynamic proline metabolism: importance and regulation in water limited environments. *Front Plant Sci* **6**, 484 (2015).
41.Z. Zhao, W. Zhang, B. A. Stanley, S. M. Assmann, Functional proteomics of Arabidopsis thaliana guard cells uncovers new stomatal signaling pathways. *Plant Cell* **20**, 3210-3226 (2008).
42.L. M. Fan *et al.*, Abscisic acid regulation of guard-cell K+ and anion channels in Gbeta- and RGS-deficient Arabidopsis lines. *Proc Natl Acad Sci U S A* **105**, 8476-8481 (2008).
43.S. Munemasa *et al.,* Mechanisms of abscisic acid-mediated control of stomatal aperture *Curr Opin Plant Biol.* 2015 Dec;28:154-62. doi: 10.1016/j.pbi.2015.10.010.
44. M.S. Hossain et al., Glucosinolate degradation products, isothiocyanates, nitriles, and thiocyanates, induce stomatal closure accompanied by peroxidase-mediated reactive oxygen species production in Arabidopsis thaliana. *Biosci Biotechnol Biochem.* 2013;77(5):977-83.
45. X. Jin et al., Abscisic acid-responsive guard cell metabolomes of Arabidopsis wild-type and gpa1 G-protein mutants. *Plant Cell.* 2013 Dec;25(12):4789-811

Acknowledgements

We thank Jiyoung Park, Po-Kai Hsu and Julian Schroeder for *abi1-1*and *ghr1* seeds and for help with stomatal aperture measurement, Eric Schmelz for assistance with freeze drying of samples, Jeongim Kim and Clint Chapple for *cyp83a1* seeds, Venkatesan Sundaresan and Titima Tantikanjana for *cyp79f* single and double mutant lines, and Jim Whelan for *wrky63-1* and *35S::WRKY63* seeds. **Funding** This work was supported by grants from the NIH (GM43644 to ME; JRE), the Howard Hughes Medical Insitute (ME and JRE), the NSF (IOS 1547796 and 1339125 to DJK) the USDA National Institute of Food and Agriculture, (Hatch project number CA-D-PLS-7033-H to DJK) and by the Danish National Research Foundation (DNRF99) grant. **Contributions.** MS and ME conceived of the project. MS prepared samples. MT analyzed RNAseq data. BL and EK performed glucosinolate assays. MS generated transgenic lines, performed genetic experiments, and performed physiological experiments. DJK assisted with glucosinolate analysis. MS and ME wrote the manuscript. MS, ME, LS, JRE, EK, and DJK edited the manuscript. JRE and LS provided materials. **Competing interests.** The authors declare no competing interests. **Data and materials availability.** Plant lines will be available through the Arabidopsis Stock Center. RNAseq data will be deposited into NCBI as GEO#xxxxx.

Supplementary Materials:

Materials and Methods

Tables S1-S3

Figures S1-S4

References 25-45

Figure Legends

Figure 1. The *iaa5,6,19* mutant has lower aliphatic glucosinolate levels after dehydration stress. (A) Aliphatic glucosinolate biosynthetic pathway. The genes listed to the right are all down-regulated in the triple mutant compared to the wild type after dehydration. (B) Heat map showing that aliphatic glucosinolate biosynthetic genes are down regulated in the *iaa5,6,19* mutant during desiccation stress. (C) Time course measurement of 4-MSO levels in 7-day-old seedlings of indicated genotypes at time intervals after application of dehydration stress. Results are presented as the means ± SE of one experiment with 6 biological replicates consisting of n=20 pooled seedlings in each. Two independent experiments showed similar trend. Statistical significance was determined by (Student's t –test). P=0.008 and 0.013 respectively for *iaa5619* at 60 and 180 minutes of desiccation.

Figure 2. Aliphatic glucosinolate deficiency is linked to decreased drought tolerance. (A) *cyp79f1, cyp79f2* single mutant and *cyp79f1f2* double mutants are less drought tolerant compared to the wild type. (B) Quantification of rosette dry weight from (A). (C) *myb28,29* double mutants are less drought tolerant compared to the wild type. (D) *35S:MYB28*, *35S:MYB29 and 35S:AOP2* plants display increase drought tolerance (E) Overexpression of *MYB28* or *MYB29* restores drought tolerance to *iaa19-1* plants. Results are presented as the means ± SE of one experiments with n=10 independent pots. Each experiment was

repeated at least twice. For panels A, C. D. and E, differences between mutants and Col-0 are significant at $p < 0.05$ (∗) and $p < 0.01$ (∗∗) by two-tailed Student's t test.

Figure 3. Drought activates a transcriptional cascade to regulate GLS biosynthetic genes. (A) Relative *WRKY63* RNA level in the *iaa5,6,19* mutants compared to wild-type seedlings before and after desiccation for one hour. (B)) IAA19 binds to a tandem repeat of *AuxRE* elements in the promoter of *WRKY63* (-350 to -361). ChIP was from the *rAA19-YPet-His-FLAG* line. Results are presented as the means ± SE of 3 independent biological experiments with 3 technical replicates in each. Statistical significance was determined by two-tailed Student's t test. **P <0.05. (C) Relative *MYB28* and *MYB29* RNA level in the seedlings of *35S:WRKY63* lines. (D) *35S:WRKY63* lines are less tolerant to drought than wild-type plants after water withholding in pots. Results are presented as the means ± SE of one independent experiments with n=10 independent pots/plants. Differences are significant at $p < 0.05$ (∗) and $p < 0.01$ (∗∗) by two-tailed Student's t test.

Figure 4. Defects in stomatal regulation are responsible for decreased drought tolerance in glucosinolate deficient mutants. (A) Stomatal response to drought in Col-0, *iaa5,6,19* and *mybn28,29* lines. **(B)** Stomatal response to application of ABA and 4-MSO in Col-0, *iaa5,6,19* and *myb28,29* **(C)** 4-MSO inhibits light-induced opening of stomata from dark-adapted plants while the indolic GLS I3M is ineffective. (**D**) Recovery of *iaa5,6,19* mutants to topical application of 4-MSO during drought stress. Results are presented as the means ± SE of one experiments with n=10 independent pots. Two independent experiments produced similar results. (**E**) Stomatal response to I3M in light-grown plants. (**F**) Response of the *abi1-1* mutant to the aliphatic GLS sinigrin hydrate. (**F**) Unlike Col-0 or *abi1-1, ghr1* does not respond to 50 µM SH. (**G**). Response of the *ghr1* mutant to 4-MSO, with *abi1-1* as a control. (**H**) 4-MSO levels in *tir1/afb* mutants after 60 min desiccation treatment. (**I**) The *tir1/afb* mutants display increased tolerance to water withholding in pots.

For stomatal closure experiments, n = 250-300 stomata from 6 different leaves from 3 different plants grown in the same chamber and growth condidtions. Results are presented as the means ± SE. Differences are significant at $p < 0.05$ (∗) and $p < 0.01$ (∗∗) by two-tailed Student's t test.

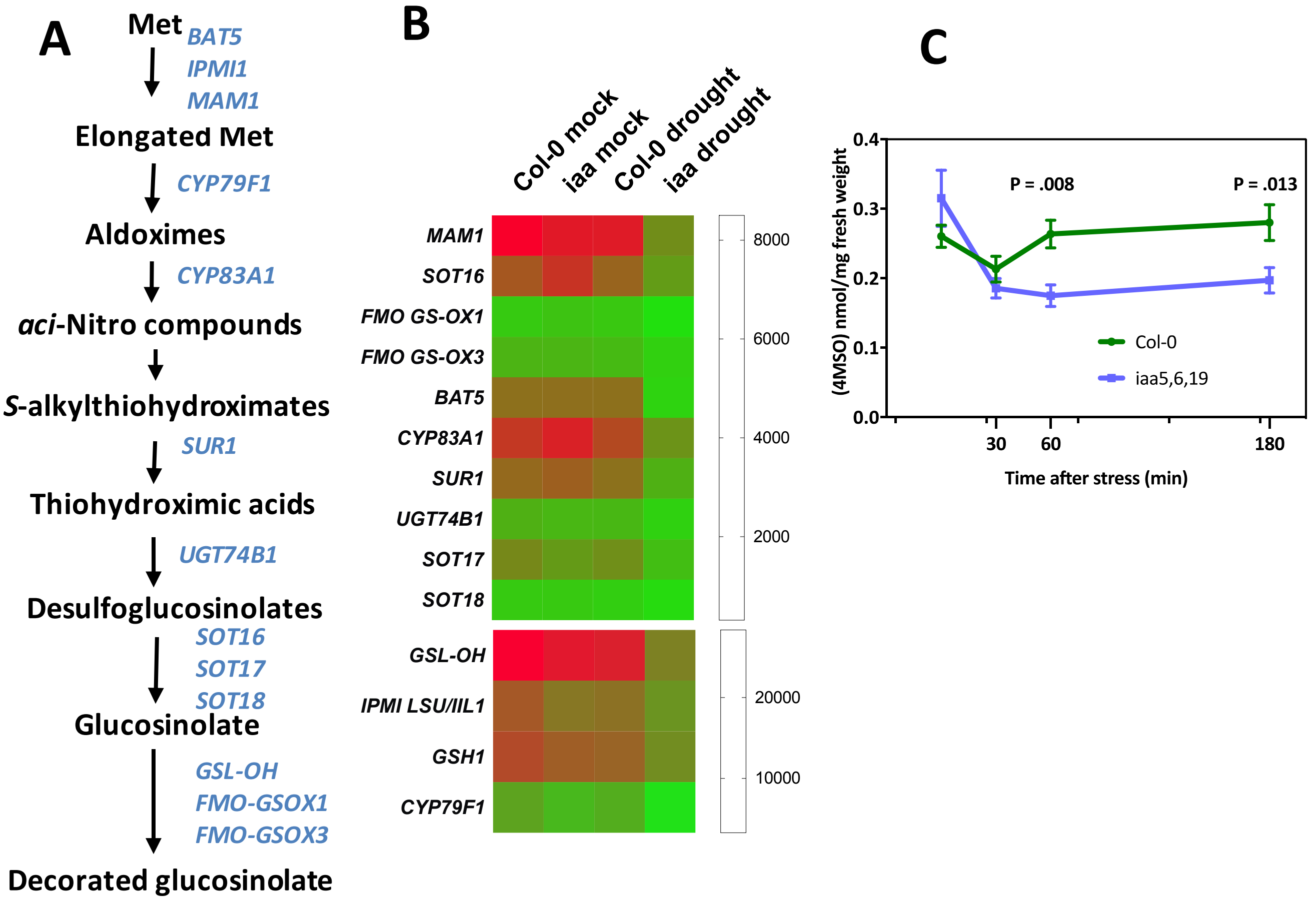
A
Met
BAT5
IPMI1
MAM1
Elongated Met
CYP79F1
Aldoximes
CYP83A1
aci-Nitro compounds
S-alkylthiohydroximates
SUR1
Thiohydroximic acids
UGT74B1
Desulfoglucosinolates
SOT16
SOT17
SOT18
Glucosinolate
GSL-OH
FMO-GSOX1
FMO-GSOX3
Decorated glucosinolate
B
Col-0 mock
iaa mock
Col-0 drought
iaa drought
MAM1
SOT16
FMO GS-OX1
FMO GS-OX3
BAT5
CYP83A1
SUR1
UGT74B1
SOT17
SOT18
8000
6000
4000
2000
GSL-OH
IPMI LSU/IIL1
GSH1
CYP79F1
20000
10000
C
(4MSO) nmol/mg fresh weight
0.4
0.3
0.2
0.1
0.0
P = .008
P = .013
Col-0
iaa5,6,19
30
60
180
Time after stress (min)

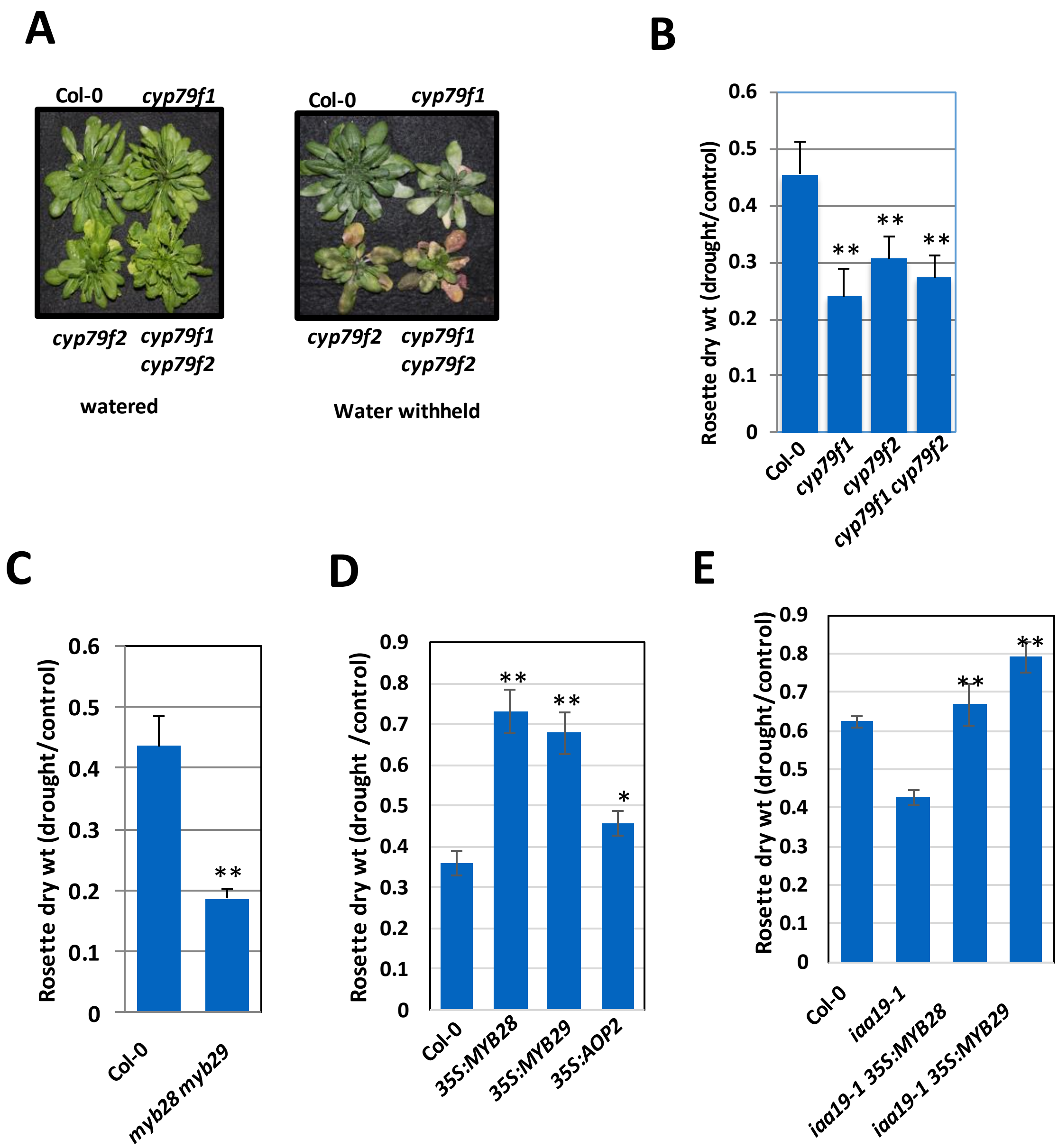
A
Col-0
cyp79f1
cyp79f2
cyp79f1 cyp79f2
watered
Water withheld
B
Rosette dry wt (drought/control)
0
0.1
0.2
0.3
0.4
0.5
0.6
**
Col-0
cyp79f1
cyp79f2
cyp79f1 cyp79f2
C
Rosette dry wt (drought/control)
Col-0
myb28 myb29
D
Rosette dry wt (drought /control)
0.7
0.8
0.9
*
35S:MYB28
35S:MYB29
35S:AOP2
E
iaa19-1
iaa19-1 35S:MYB28
iaa19-1 35S:MYB29

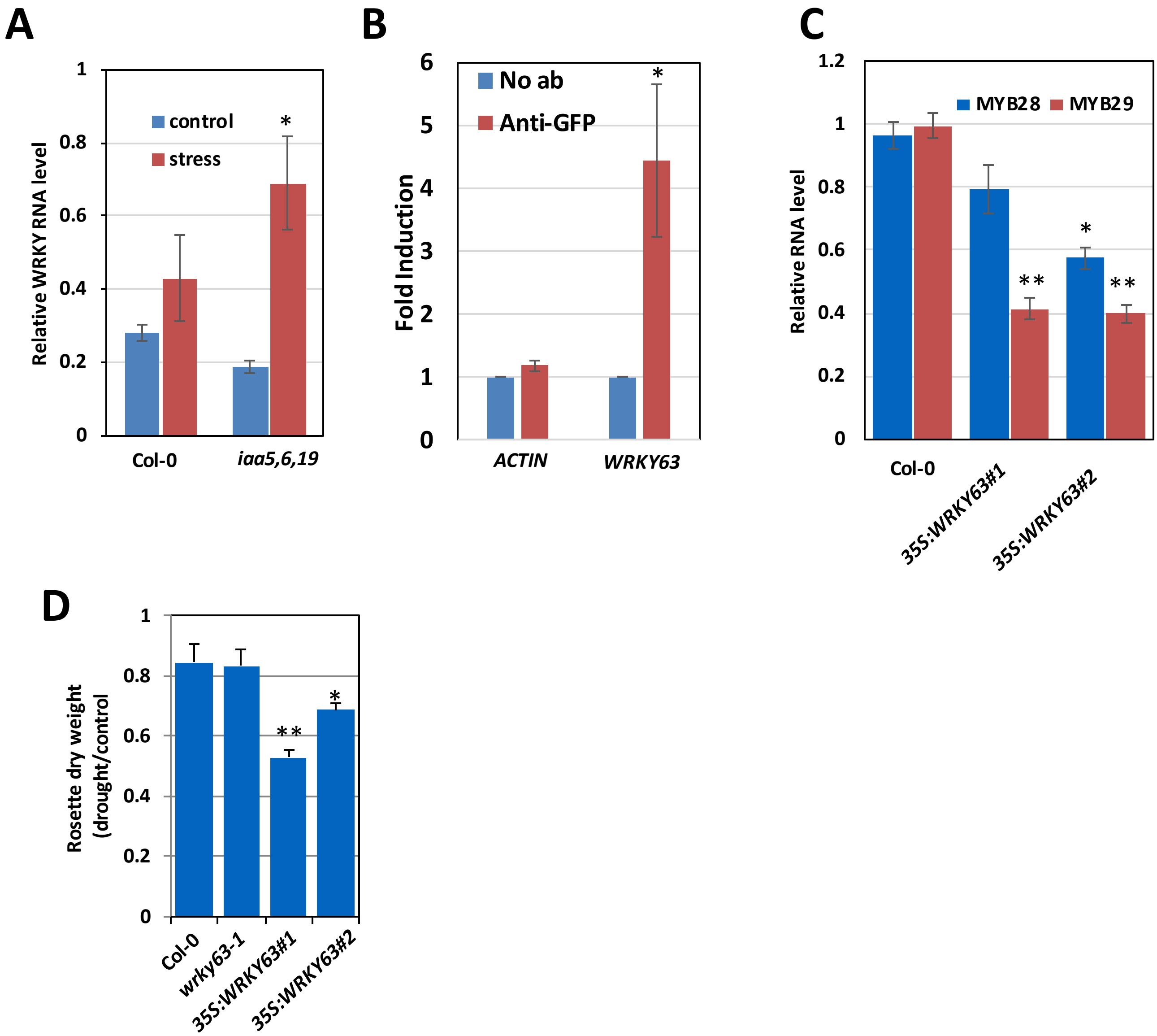
A
Relative WRKY RNA level
control
stress
*
Col-0
iaa5,6,19
B
Fold Induction
No ab
Anti-GFP
*
ACTIN
WRKY63
C
Relative RNA level
MYB28
MYB29
*
**
**
Col-0
35S:WRKY63#1
35S:WRKY63#2
D
Rosette dry weight
(drought/control)
**
*
Col-0
wrky63-1
35S:WRKY63#1
35S:WRKY63#2

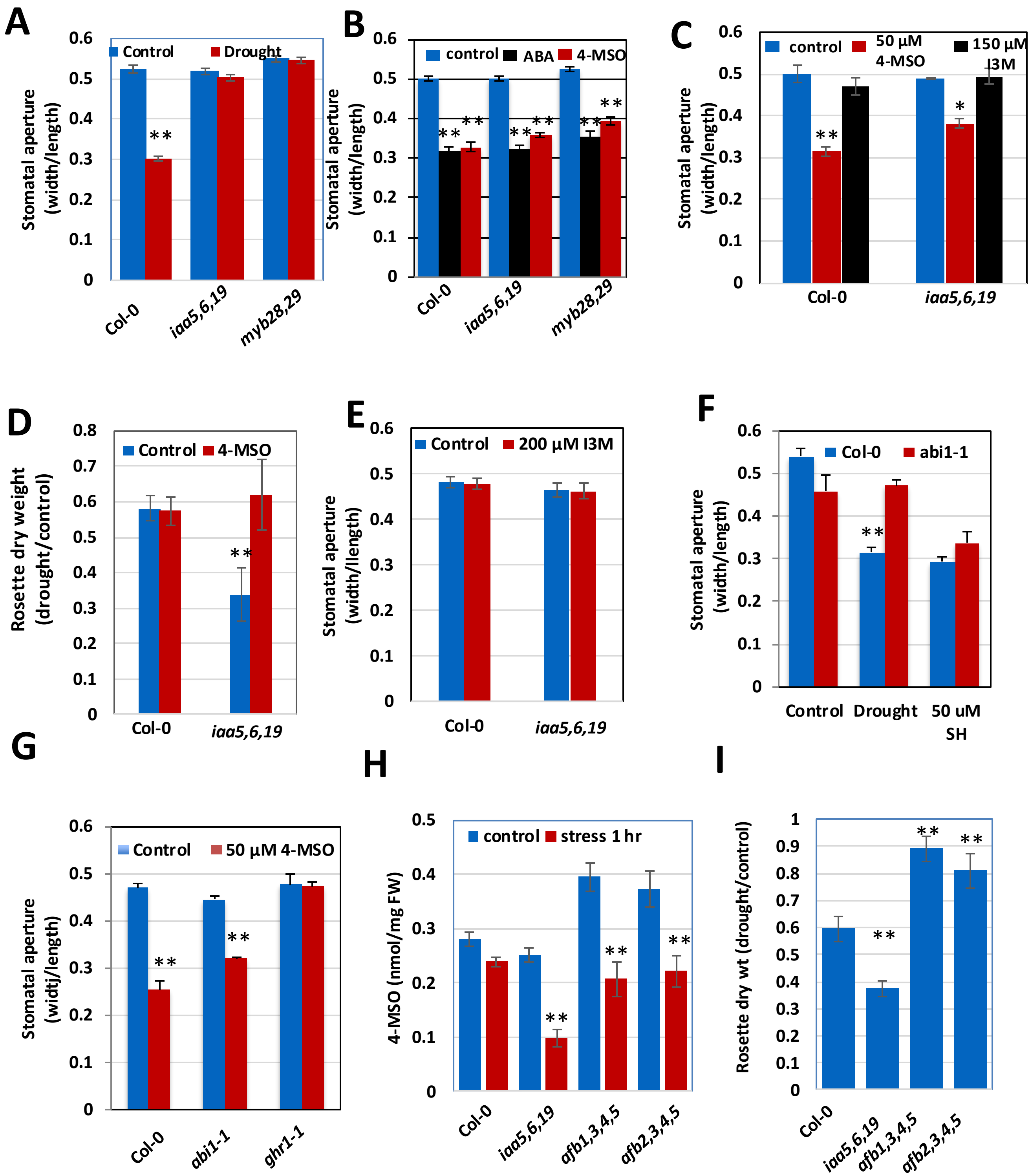
A
Control
Drought
Stomatal aperture (width/length)
0.6
0.5
0.4
0.3
0.2
0.1
0
**
Col-0
iaa5,6,19
myb28,29
B
control
ABA
4-MSO
Stomatal aperture (width/length)
Col-0
iaa5,6,19
myb28,29
C
control
50 µM 4-MSO
150 µM I3M
Stomatal aperture (width/length)
Col-0
iaa5,6,19
D
Control
4-MSO
Rosette dry weight (drought/control)
Col-0
iaa5,6,19
E
Control
200 µM I3M
Stomatal aperture (width/llength)
Col-0
iaa5,6,19
F
Col-0
abi1-1
Stomatal aperture (width/length)
Control
Drought
50 uM SH
G
Control
50 µM 4-MSO
Stomatal aperture (widtj/length)
Col-0
abi1-1
ghr1-1
H
control
stress 1 hr
4-MSO (nmol/mg FW)
Col-0
iaa5,6,19
afb1,3,4,5
afb2,3,4,5
I
Rosette dry wt (drought/control)
Col-0
iaa5,6,19
afb1,3,4,5
afb2,3,4,5

Materials and Methods

Plant Materials and Growth Conditions

Arabidopsis thaliana seed were sterilized with chlorine fumes generated by mixing 49 ml bleach and 1 ml hydrochloric acid. Sterilized seeds were sown on ½ strength MS media, stratified at 4^0C for 2-3 days, and grown in long day conditions (16 h light: 8 h dark) at 22 ^{0}C with a light intensity of ~110-130 µmol m^{-2} sec^{-1}. In addition to wild type Col-0 and Ws lines, the following mutant lines were used as described: *iaa19-1* and *iaa5 iaa6 iaa19, dreb2a dreb2b(3)*; *cyp79f1 cyp79f2 (3)*; *myb28 myb29*, *35S:MYB28, 35S:MYB29* (*26*); *35S:WRKY63* OE *(27). abi1-1(28). ghr1(29).*

Plasmid Construction

rIAA19-YPet-His-Flag was constructed by recombineering a 1xYPet-6xHis-3xFlag tag to the C-terminus of the IAA19 gene in the Arabidopsis TAC clone JAtY59D10. The cloning procedure and the tag sequence have been previously described (*3, 30*)

Transgenic Plants

After floral dip of wild-type Col-0 plants (*31*), single-insertional transgenic lines of rIAA19-YPet-His-Flag were selected by chi-square test from T2 plants on 1x Linsmaier & Skoog (Caisson Labs, UT) plates containing 15 mg/ml glufosinate ammonium. The expression of the tagged TFs was confirmed by Western blotting. Homozygous transgenic lines were selected from the subsequent generation for bulking seeds.

RNAseq

Col-0 and *iaa5,6,19* seedlings were grown on ½ MS for 7 days and desiccated for 1 h on parafilm at room temperature. Total RNA was extracted from three independent biological replicates of each genotype using RNeasy Plant Mini Kits (Cat#79254, Qiagen, CA) and genomic DNA contamination was removed by digestion with Turbo DNase (Cat# AM1907, BioRad, CA) and/or RNase-Free DNase (Cat#79254, Qiagen). RNA quantity was checked by Bioanalyzer for quality control. Library construction and sequencing were performed at the IGM genomics center at UCSD. About 40 million reads were obtained for each sample. Raw reads were processed at Bioinformatics core facility, UCSD School of Medicine using Array Studio software. Alignments were performed using OSA4 and differential expression determined using DESeq2 (*32*). Gene ontology analysis was performed using Panther (*33-35*). Raw reads were submitted into NCBI as GEO#xxxxx.

ChIP qPCR

For ChIP qPCR Col-0, *recIAA19: YPet-His-FLAG* and *gWRKY63: WRKY63: eYFP* plants were grown on ½ MS for 7 days in the dark. Approximately 1g tissues were collected and crosslinked with Pierce™ Methanol-free 16% Formaldehyde (w/v) (Cat#28906, Thermo Fischer Scientific, Carlsbad, CA) diluted to 1%, for 20 minutes and quenched with 2M glycine for 5 minutes. Samples were flash frozen and ground in liquid nitrogen. Chromatin was prepared using EpiQuik

Plant ChIP Kit (Cat# P-2014-48, NY, USA) as per manufacturer's instructions. Chromatin was sheared at 4^0C by 16 cycles of 30sec on and 90sec off on high settings using Bioruptor Plus sonicator device (Cat# B01020002, Diagenode, US). IP was done with anti-GFP antibody (Cat#A111222, Thermo Fischer, Carlsbad) at 4^0C overnight. Purified DNA was used for qRT-PCR using SYBR green dye in a CFX96 Real-Time System (Bio-Rad, Hercules, CA).

RT qPCR

Total RNA was extracted using RNA RNeasy Plant Mini Kits (Cat#79254, Qiagen) and genomic DNA contamination was removed by digestion with Turbo DNase (Cat# AM1907, BioRad, CA) and/or RNase-Free DNase (Cat#79254, Quiagen). cDNA was synthesized using SuperScript III (Cat# 18080085, Life Technologies/Thermo Fischer, Carlsbad) and analyzed by quantitative PCR using PowerUp™ SYBR® Green Master Mix (Cat#A25742, Thermo Fischer Scientific, Carlsbad, CA) on a CFX96 Real-Time System (Biorad, Hercules, CA). RNA levels were normalized against PP2A gene. Fold induction was calculated by ddCt method (*36*) and RNA levels as previously described (*37*). The oligos used for PCR are listed in Supplementary Table 3.

Glucosinolate Profiling

Blind experiments were conducted with 3 different genotypes as described above. For each assay 2 independent experiments with 6 independent biological replicates grown under same condition were used. Typically, 20-30mg (fresh weight) of pooled 7 day-post-germination seedlings (n=15-20) were sampled, freeze dried and sent to UC Davis at room temperature for GLS quantification. 400 µl 90% (v/v) methanol was added to each sample tube and stored at -20°C before extraction. The tissues were disrupted with two 2.3 mm metal ball bearings in a paint shaker at room temperature and incubated at room temperature for 1 hour. Tissues were pelleted by centrifugation for 15 minutes at 2500 g and the supernatant was used for anion exchange chromatography in 96-well filter plates. After methanol and water washing steps, the columns were incubated with sulfatase solution overnight. Desulfo-GLS were eluted and analyzed by HPLC according to a previously described method (*38*).

Drought Stress Assays

Osmotic stress assays were performed as described in (*3*). Briefly 35 ml ½ MS media with 1% sucrose and 0.8% Bactoagar was autoclaved and solidified in 120 mm square plates and perfused overnight with 50 ml 30% filter sterilized PEG-8000 solution. PEG was drained the next day. 5-6 day-post-germination seedlings were transferred to either ½-MS or ½-MS+PEG plates and incubated at 22 ^{0}C in long days. Root length and plant fresh weight were measured after 8 to 10 days.

Drought stress assays in soil were performed as described in done as described (*39,40*) with minor modifications. 7 to 10-day-old seedlings were planted in sectors (two plants per sector) of 8 cm × 8 cm × 10 cm (L × W × H) plastic pots. Plants were grown in a short-day chamber (8h/16 hr. light/dark) at 21 ^{0}C during day 18 ^{0}C during night with light intensity of 110–130 µmol m⁻

^{2} sec^{-1}. Seedlings were fertilized regularly. After 18-20 days, pots were saturated with water, drained and weighed. Subsequently, water was withheld for 18-22 days to reduce weight up to 50% and each pot was re-watered to 75% level by injecting 40-50 ml of water in the middle of the pot with a 22-gauge needle. Pots were then subjected to re-drought for 12-15 days to reduce pot weight to 50-60%. Fresh weight and dry-weights of each rosette were measured. For dry weight rosettes were dried overnight at 65^{0}C in a hot air oven.

In the experiments to determine the effects of GLS on drought tolerance, plants were treated as above except that water withholding began after two weeks of watering. At the same time, plants were sprayed with 50 uM 4-MSO, 50 µM sinigrin hydrate or water 6 times during the first over the next 10 to 12 days.

Stomata Aperture Measurement

Stomatal aperture experiments were performed using fully expanded young leaves from wild-type and mutant plants grown for 3-4 weeks in a growth room with 8 h of light/16 h of dark. To determine the effects of GLSs and drought on stomatal closure, control plants and plants that were subjected to water withdrawal for 3-4 days were placed in the light overnight to open the stomata. Leaves were then incubated in closing solution (5 mM MES-KOH [pH 6.15], 20mM KCl, and 1mM $CaCl_2$) under light (110-130 mmol/m2/s) for 2.5 h followed by a further 2.5 h in the presence of 50 uM 4-MSO (Glucoraphanin, Cat# 0009445, Cayman Chemicals), 200 uM I3M (Cat# 2503S, Alkemist Labs), or 20 uM ABA. Abaxial leaf epidermal peels were fixed on glass slide with coverslips as described previously (*41,42*) using Hollister Medical Adhesive Spray. Stomatal apertures were measured with a light microscope (Nikon, Japan). The epidermal peels were examined under a 40x objective using the microscope. After image acquisition, widths and lengths of stomatal apertures were measured using the ImageJ software (NIH, Bethesda, US). Six independent biological replicates (40-50 stomata from one seedling per replicate) were used for one experiment and at least three independent plants were used.

To determine the effects of GLS on stomatal opening, leaves were incubated in opening solution (10 mM MES-KOH [pH 6.15], 10mM KCl, and 10 mM iminodiacetic acid) in the dark for 2.5 h with their adaxial surface upward. Upon transfer to the light, 50uM 4-MSO, 50uM sinigrin hydrate (Cat# S1647, Sigma-Aldrich) 200 µM I3M or 20 µM ABA were added to the solution. Stomatal aperture was measured as above.

Statistical Analysis

GraphPad Prism 5.0 (San Diego, CA) and Microsoft Excel 2008 were utilized for preparing graphs and statistical analysis. ANOVA utilized for GLS analysis. For others two tailed t-tests were employed.

Table S1. Genes differentially regulated in iaa5,5,19 vs Col-0

Down-regulated genes *iaa5,6,19* vs Col-0 during stress (FDR < 0.001

GeneID	Genotype =>	Genotype =>	Genotype => iaa5	Genotype => iaa561	GeneName
AT1G53480	-4.194	-18.3032	1.60E-143	4.22E-139	MRD1
AT1G54110	-2.1168	-4.3374	3.04E-38	4.01E-34	AT1G54110
AT3G30180	-1.2249	-2.3374	3.55E-25	3.12E-21	CYP85A2
AT3G15540	-1.815	-3.5187	9.65E-25	6.36E-21	IAA19
AT5G23010	-1.0287	-2.0403	1.11E-23	4.90E-20	MAM1
AT1G19200	-1.5696	-2.9683	1.63E-20	5.38E-17	AT1G19200
AT5G53048	-1.5212	-2.8702	2.85E-20	8.35E-17	AT5G53048
AT3G52840	-0.9455	-1.9259	6.26E-19	1.65E-15	BGAL2
AT4G35770	-1.2253	-2.338	1.04E-18	2.49E-15	STR15
AT4G04223	-1.5615	-2.9517	1.85E-18	4.08E-15	AT4G04223
AT3G17790	-1.345	-2.5404	7.50E-18	1.52E-14	PAP17
AT3G56040	-0.9606	-1.9461	2.84E-17	5.36E-14	UGP3
AT1G52190	-1.0205	-2.0286	5.32E-17	9.36E-14	NPF1.2
AT4G31500	-1.2267	-2.3403	7.42E-17	1.22E-13	CYP83B1
AT2G05540	-1.2492	-2.3771	1.25E-16	1.94E-13	AT2G05540
AT5G20150	-1.0159	-2.0221	1.72E-16	2.52E-13	SPX1
AT5G01220	-1.1999	-2.2972	3.38E-15	4.24E-12	SQD2
AT5G20790	-1.4151	-2.6667	3.96E-15	4.54E-12	AT5G20790
AT4G14040	-0.7694	-1.7045	7.35E-15	7.71E-12	SBP2
AT1G70890	-0.7759	-1.7122	7.12E-15	7.71E-12	MLP43
AT3G02020	-1.0689	-2.0978	9.76E-15	9.54E-12	AK3
AT1G68670	-0.855	-1.8088	1.29E-14	1.18E-11	AT1G68670
AT4G30270	-0.9145	-1.8849	1.26E-14	1.18E-11	XTH24
AT1G49500	-1.1023	-2.1469	1.38E-14	1.21E-11	AT1G49500
AT3G21250	-0.7278	-1.6562	1.77E-14	1.42E-11	ABCC8
AT3G01970	-1.1369	-2.199	2.24E-14	1.69E-11	WRKY45
AT5G20410	-1.2793	-2.4272	2.24E-14	1.69E-11	MGD2
AT3G03470	-1.1735	-2.2555	2.91E-14	2.07E-11	CYP89A9
AT3G57520	-0.9571	-1.9414	3.34E-14	2.32E-11	RFS2
AT4G03060	-1.3704	-2.5855	3.47E-14	2.34E-11	AOP2
AT2G27190	-0.7821	-1.7196	4.57E-14	3.01E-11	PAP12
AT5G63160	-0.9391	-1.9174	6.23E-14	3.82E-11	BT1
AT4G37800	-0.9326	-1.9087	8.90E-14	5.22E-11	XTH7
AT3G23050	-0.7574	-1.6904	9.52E-14	5.34E-11	IAA7
AT4G39940	-1.12	-2.1735	1.27E-13	6.97E-11	APK2
AT4G23680	-1.217	-2.3246	1.38E-13	7.45E-11	AT4G23680
AT2G20670	-1.3349	-2.5226	1.52E-13	8.03E-11	AT2G20670
AT2G20610	-0.9792	-1.9714	1.61E-13	8.34E-11	SUR1
AT4G16690	-0.9465	-1.9272	1.94E-13	9.67E-11	PPD
AT2G25450	-0.7605	-1.694	3.06E-13	1.50E-10	GSL-OH
AT3G02040	-1.2044	-2.3044	3.17E-13	1.52E-10	GDPD1
AT4G08290	-0.993	-1.9904	3.46E-13	1.60E-10	AT4G08290

AT5G19120	-1.2055	-2.3062	4.28E-13	1.94E-10	AT5G19120
AT4G13770	-0.9939	-1.9916	7.09E-13	3.08E-10	CYP83A1
AT1G75460	-0.8302	-1.7779	7.91E-13	3.37E-10	AT1G75460
AT1G27020	-0.789	-1.7279	9.20E-13	3.83E-10	AT1G27020
AT4G12030	-0.8794	-1.8396	9.70E-13	3.94E-10	BASS5
AT3G47420	-1.0083	-2.0116	1.21E-12	4.77E-10	ATPS3
AT5G63800	-0.7207	-1.648	1.96E-12	7.62E-10	BGAL6
AT4G33030	-0.7124	-1.6385	2.56E-12	9.65E-10	SQD1
AT2G36970	-1.1165	-2.1682	2.53E-12	9.65E-10	UGT86A1
AT4G19160	-0.7672	-1.702	2.81E-12	1.03E-09	AT4G19160
AT2G36800	-0.9759	-1.9669	3.90E-12	1.41E-09	UGT73C5
AT4G32480	-1.1858	-2.2749	5.68E-12	2.02E-09	AT4G32480
AT5G57780	-1.0368	-2.0516	5.78E-12	2.03E-09	AT5G57780
AT5G64620	-0.9447	-1.9247	7.02E-12	2.44E-09	C/VIF2
AT3G15630	-0.9128	-1.8827	1.56E-11	5.28E-09	AT3G15630
AT5G41080	-1.155	-2.2269	1.76E-11	5.87E-09	GDPD2
AT1G79410	-0.6954	-1.6194	2.05E-11	6.68E-09	OCT5
AT2G46650	-0.8423	-1.793	2.65E-11	8.51E-09	CYTB5-C
AT4G34950	-0.91	-1.8791	2.75E-11	8.73E-09	AT4G34950
AT4G04040	-0.6083	-1.5244	3.74E-11	1.17E-08	PFP-BETA2
AT3G15450	-1.1233	-2.1784	3.87E-11	1.20E-08	AT3G15450
AT3G21690	-0.712	-1.6381	4.24E-11	1.28E-08	AT3G21690
AT1G16390	-1.1929	-2.2861	4.42E-11	1.32E-08	OCT3
AT4G35750	-0.9471	-1.928	5.35E-11	1.58E-08	AT4G35750
AT3G14210	-0.6163	-1.533	5.73E-11	1.68E-08	ESM1
AT1G71030	-1.1638	-2.2404	6.49E-11	1.88E-08	ATMYBL2
AT2G41940	-0.9462	-1.9267	6.60E-11	1.89E-08	ZFP8
AT3G48310	-0.6054	-1.5214	7.64E-11	2.17E-08	CYP71A22
AT4G15540	-0.8257	-1.7724	1.01E-10	2.80E-08	AT4G15540
AT4G24230	-0.9828	-1.9763	1.00E-10	2.80E-08	ACBP3
AT3G58990	-0.9893	-1.9852	1.06E-10	2.92E-08	IPMI1
AT3G44880	-0.6791	-1.6012	1.08E-10	2.93E-08	PAO
AT4G24350	-0.9772	-1.9686	1.21E-10	3.25E-08	AT4G24350
AT4G37310	-0.6981	-1.6224	1.57E-10	4.13E-08	CYP81H1
AT2G30520	-0.9863	-1.9811	2.28E-10	5.90E-08	RPT2
AT5G07100	-0.8285	-1.7758	2.43E-10	6.22E-08	WRKY26
AT1G54740	-0.801	-1.7423	2.59E-10	6.56E-08	AT1G54740
AT3G55240	-0.9272	-1.9015	2.77E-10	6.94E-08	AT3G55240
AT2G22330	-0.7279	-1.6562	3.49E-10	8.52E-08	CYP79B3
AT1G02820	-1.0731	-2.104	3.52E-10	8.52E-08	AT1G02820
AT3G26280	-0.7492	-1.6808	3.70E-10	8.87E-08	CYP71B4
AT2G05380	-0.7736	-1.7095	4.27E-10	1.02E-07	GRP3S
AT5G44020	-0.8544	-1.8081	4.53E-10	1.07E-07	AT5G44020
AT1G77760	-0.8702	-1.8279	4.71E-10	1.10E-07	NIA1
AT3G07350	-1.1096	-2.1579	4.76E-10	1.10E-07	AT3G07350

AT3G30775	-0.9802	-1.9727	5.19E-10	1.18E-07	POX1
AT1G17710	-1.1248	-2.1807	5.17E-10	1.18E-07	AT1G17710
AT1G74100	-0.924	-1.8973	5.36E-10	1.21E-07	SOT16
AT1G65860	-1.115	-2.166	5.98E-10	1.33E-07	FMOGS-OX1
AT2G14750	-0.9656	-1.9528	6.53E-10	1.43E-07	APK1
AT1G53490	-0.929	-1.904	7.57E-10	1.65E-07	HEI10
AT3G62820	-0.6668	-1.5876	8.06E-10	1.74E-07	AT3G62820
AT3G26510	-1.0496	-2.0699	9.56E-10	2.03E-07	AT3G26510
AT5G65730	-1.0862	-2.1231	1.04E-09	2.19E-07	XTH6
AT5G57630	-0.6874	-1.6104	1.10E-09	2.30E-07	CIPK21
AT1G23870	-0.7446	-1.6755	1.11E-09	2.30E-07	TPS9
AT3G50480	-0.7704	-1.7058	1.11E-09	2.30E-07	HR4
AT2G31790	-0.7402	-1.6704	1.22E-09	2.50E-07	UGT74C1
AT5G14780	-0.7402	-1.6704	1.23E-09	2.50E-07	FDH1
AT2G22990	-0.6156	-1.5322	1.32E-09	2.66E-07	SCPL8
AT1G27290	-0.7169	-1.6436	1.38E-09	2.76E-07	AT1G27290
AT1G25440	-0.8775	-1.8372	1.41E-09	2.80E-07	COL16
AT2G26660	-0.7201	-1.6473	1.50E-09	2.96E-07	SPX2
AT5G22390	-0.7819	-1.7194	1.55E-09	3.03E-07	AT5G22390
AT1G15260	-0.8885	-1.8513	1.78E-09	3.45E-07	AT1G15260
AT3G26170	-1.035	-2.0492	1.93E-09	3.72E-07	CYP71B19
AT2G25080	-0.5921	-1.5075	2.19E-09	4.18E-07	GPX1
AT2G19800	-0.9106	-1.8798	2.24E-09	4.26E-07	MIOX2
AT1G33811	-0.7703	-1.7056	2.33E-09	4.36E-07	AT1G33811
AT2G34210	-1.0102	-2.0143	2.42E-09	4.50E-07	AT2G34210
AT4G15530	-0.7261	-1.6541	2.48E-09	4.57E-07	PPDK
AT3G59930	-1.0692	-2.0983	2.70E-09	4.91E-07	AT3G59930
AT4G04840	-1.0483	-2.0681	2.74E-09	4.95E-07	MSRB6
AT3G54600	-0.7661	-1.7006	3.07E-09	5.51E-07	DJ1F
AT1G62380	-0.6118	-1.5282	3.11E-09	5.54E-07	ACO2
AT1G52100	-0.8392	-1.789	3.23E-09	5.72E-07	AT1G52100
AT2G46220	-0.6212	-1.5382	3.38E-09	5.86E-07	AT2G46220
AT5G02480	-0.6456	-1.5644	3.36E-09	5.86E-07	AT5G02480
AT4G38470	-0.7815	-1.7189	3.60E-09	6.21E-07	AT4G38470
AT1G15100	-0.6742	-1.5957	3.71E-09	6.36E-07	RHA2A
AT5G07460	-0.8677	-1.8247	3.79E-09	6.42E-07	MRSA2
AT4G37610	-0.8947	-1.8592	3.79E-09	6.42E-07	BT5
AT3G51600	-0.6923	-1.6159	4.01E-09	6.68E-07	LTP5
AT5G56550	-1.0004	-2.0006	4.02E-09	6.68E-07	OXS3
AT1G68740	-0.6326	-1.5503	4.36E-09	7.19E-07	PHO1-H1
AT4G16680	-0.6366	-1.5547	5.11E-09	8.32E-07	AT4G16680
AT5G15410	-0.8769	-1.8364	5.68E-09	8.98E-07	CNGC2
AT2G06850	-0.659	-1.579	5.82E-09	9.14E-07	XTH4
AT3G04110	-0.6751	-1.5967	7.05E-09	1.09E-06	GLR1.1
AT4G16880	-0.898	-1.8635	7.83E-09	1.19E-06	AT4G16880

AT1G24100	-0.9108	-1.88	8.57E-09	1.29E-06	UGT74B1
AT3G42658	-1.0167	-2.0232	9.20E-09	1.38E-06	SADHU3-2
AT4G10120	-0.8717	-1.8298	9.45E-09	1.40E-06	SPS4
AT5G27350	-0.6695	-1.5905	9.64E-09	1.42E-06	SFP1
AT4G21680	-0.9697	-1.9585	1.04E-08	1.53E-06	NPF7.2
AT3G28740	-1.0071	-2.0099	1.08E-08	1.58E-06	CYP81D11
AT5G47610	-0.8201	-1.7655	1.12E-08	1.61E-06	ATL79
AT4G19170	-0.9953	-1.9936	1.16E-08	1.65E-06	CCD4
AT1G18810	-0.8642	-1.8204	1.19E-08	1.69E-06	PKS3
AT1G64900	-0.7619	-1.6958	1.25E-08	1.77E-06	CYP89A2
AT1G17830	-0.7329	-1.662	1.35E-08	1.88E-06	AT1G17830
AT5G64570	-0.9411	-1.92	1.34E-08	1.88E-06	BXL4
AT5G53030	-0.8971	-1.8623	1.38E-08	1.91E-06	AT5G53030
AT1G75220	-0.6681	-1.589	1.39E-08	1.91E-06	AT1G75220
AT4G15760	-0.795	-1.735	1.52E-08	2.07E-06	MO1
AT1G78230	-0.8072	-1.7498	1.65E-08	2.23E-06	AT1G78230
AT1G13990	-0.6142	-1.5307	1.70E-08	2.28E-06	AT1G13990
AT2G02950	-0.9039	-1.8711	1.81E-08	2.43E-06	PKS1
AT3G16770	-0.8264	-1.7732	1.90E-08	2.53E-06	RAP2-3
AT2G11810	-0.9914	-1.9881	1.98E-08	2.62E-06	MGD3
AT3G50750	-0.7803	-1.7175	2.11E-08	2.77E-06	BEH1
AT1G11820	-0.597	-1.5125	2.26E-08	2.96E-06	AT1G11820
AT1G09240	-1.0109	-2.0151	2.33E-08	3.03E-06	NAS3
AT5G08370	-0.5887	-1.5039	2.36E-08	3.05E-06	AGAL2
AT5G23730	-0.7403	-1.6705	2.40E-08	3.08E-06	RUP2
AT5G54630	-0.8518	-1.8047	2.40E-08	3.08E-06	AT5G54630
AT2G32540	-0.8379	-1.7875	2.64E-08	3.33E-06	CSLB4
AT3G13110	-0.8295	-1.777	2.93E-08	3.63E-06	SAT3
AT3G59300	-0.633	-1.5508	2.92E-08	3.63E-06	AT3G59300
AT5G18630	-0.7603	-1.6938	3.04E-08	3.73E-06	AT5G18630
AT3G11670	-0.7274	-1.6557	3.20E-08	3.87E-06	DGD1
AT3G16520	-0.6701	-1.5912	3.27E-08	3.94E-06	UGT88A1
AT1G18590	-0.8279	-1.7751	3.33E-08	3.98E-06	SOT17
AT5G48490	-0.9082	-1.8767	3.38E-08	4.00E-06	AT5G48490
AT1G12240	-0.8302	-1.7779	3.49E-08	4.11E-06	BFRUCT4
AT1G68520	-0.9292	-1.9043	3.72E-08	4.36E-06	COL6
AT5G41761	-0.9035	-1.8706	3.88E-08	4.53E-06	AT5G41761
AT1G21060	-0.7479	-1.6794	3.98E-08	4.63E-06	AT1G21060
AT1G80440	-0.9765	-1.9676	4.08E-08	4.72E-06	AT1G80440
AT4G15690	-0.8737	-1.8324	4.38E-08	5.03E-06	GRXS5
AT5G52250	-0.7323	-1.6613	5.74E-08	6.47E-06	RUP1
AT1G54010	-0.73	-1.6586	6.23E-08	6.90E-06	GLL23
AT5G19230	-0.7798	-1.7169	6.22E-08	6.90E-06	AT5G19230
AT5G03120	-0.8575	-1.8119	6.54E-08	7.22E-06	AT5G03120
AT2G03980	-0.7297	-1.6583	6.98E-08	7.64E-06	AT2G03980

AT1G24148	-0.7283	-1.6567	8.03E-08	8.54E-06	AT1G24148
AT2G19650	-0.6426	-1.5611	8.28E-08	8.74E-06	AT2G19650
AT2G29420	-0.5872	-1.5023	8.27E-08	8.74E-06	GSTU7
AT4G34350	-0.6441	-1.5628	1.02E-07	1.06E-05	ISPH
AT3G15510	-0.9214	-1.8939	1.03E-07	1.07E-05	ATNAC2
AT1G65870	-0.9438	-1.9237	1.14E-07	1.18E-05	DIR21
AT1G24260	-0.948	-1.9292	1.17E-07	1.20E-05	SEP3
AT5G44130	-0.853	-1.8062	1.21E-07	1.24E-05	FLA13
AT5G49740	-0.829	-1.7764	1.23E-07	1.24E-05	FRO7
AT1G62560	-0.8649	-1.8212	1.33E-07	1.33E-05	FMOGS-OX3
AT5G05730	-0.7419	-1.6724	1.36E-07	1.36E-05	ASA1
AT1G68110	-0.8292	-1.7767	1.67E-07	1.64E-05	AT1G68110
AT5G37260	-0.7	-1.6245	1.75E-07	1.71E-05	RVE2
AT2G38940	-0.7405	-1.6707	1.77E-07	1.73E-05	PHT1-4
AT4G24040	-0.7597	-1.6932	1.81E-07	1.76E-05	TRE1
AT3G05630	-0.9124	-1.8822	1.94E-07	1.87E-05	PLDP2
AT4G12290	-0.6189	-1.5357	2.16E-07	2.03E-05	AT4G12290
AT2G41250	-0.8355	-1.7845	2.21E-07	2.07E-05	AT2G41250
AT5G63980	-0.625	-1.5422	2.45E-07	2.29E-05	SAL1
AT5G13770	-0.6415	-1.5599	2.47E-07	2.29E-05	AT5G13770
AT4G15670	-0.8805	-1.841	2.80E-07	2.56E-05	GRXS7
AT3G22740	-0.9266	-1.9008	2.92E-07	2.65E-05	HMT3
AT3G10420	-0.7733	-1.7091	3.14E-07	2.83E-05	SPD1
AT1G55960	-0.8588	-1.8136	3.22E-07	2.87E-05	AT1G55960
AT1G60140	-0.6187	-1.5355	3.28E-07	2.90E-05	TPS10
AT5G64572	-0.7566	-1.6895	3.31E-07	2.92E-05	AT5G64572
AT3G06750	-0.5895	-1.5047	3.40E-07	2.98E-05	AT3G06750
AT4G21470	-0.6298	-1.5474	3.46E-07	3.02E-05	FHY
AT2G16280	-0.664	-1.5845	4.55E-07	3.86E-05	KCS9
AT4G01680	-0.7539	-1.6864	4.54E-07	3.86E-05	MYB55
AT1G58180	-0.6963	-1.6204	4.75E-07	3.99E-05	BCA6
AT5G40890	-0.7051	-1.6303	5.07E-07	4.23E-05	CLC-A
AT3G03790	-0.7683	-1.7033	5.14E-07	4.25E-05	AT3G03790
AT1G24800	-0.9033	-1.8703	5.13E-07	4.25E-05	AT1G24800
AT1G74290	-0.8982	-1.8637	6.19E-07	5.06E-05	AT1G74290
AT5G18670	-0.7378	-1.6676	6.24E-07	5.08E-05	BAM9
AT1G74090	-0.6919	-1.6155	6.40E-07	5.19E-05	SOT18
AT1G23110	-0.8803	-1.8407	6.45E-07	5.22E-05	AT1G23110
AT4G24890	-0.8966	-1.8616	6.65E-07	5.37E-05	PAP24
AT4G15700	-0.8366	-1.7859	6.78E-07	5.43E-05	GRXS3
AT3G59940	-0.5882	-1.5033	7.73E-07	6.09E-05	SKIP20
AT1G16410	-0.8647	-1.821	8.29E-07	6.45E-05	CYP79F1
AT1G70290	-0.6155	-1.5321	8.45E-07	6.54E-05	TPS8
AT3G52060	-0.6501	-1.5693	8.97E-07	6.92E-05	AT3G52060
AT3G51860	-0.6744	-1.5959	9.37E-07	7.20E-05	CAX3

AT2G39920	-0.773	-1.7088	9.84E-07	7.54E-05	AT2G39920
AT3G59400	-0.6651	-1.5857	1.06E-06	8.07E-05	GUN4
AT5G16370	-0.7736	-1.7095	1.10E-06	8.27E-05	AAE5
AT1G25400	-0.6975	-1.6217	1.15E-06	8.61E-05	AT1G25400
AT1G21460	-0.8338	-1.7823	1.16E-06	8.62E-05	SWEET1
AT3G28540	-0.7201	-1.6473	1.22E-06	8.97E-05	AT3G28540
AT1G75960	-0.7631	-1.6971	1.25E-06	9.17E-05	AAE8
AT4G12320	-0.6411	-1.5596	1.26E-06	9.17E-05	CYP706A6
AT5G45430	-0.6521	-1.5714	1.25E-06	9.17E-05	AT5G45430
AT3G26200	-0.8729	-1.8314	1.31E-06	9.50E-05	CYP71B22
AT3G48740	-0.6048	-1.5208	1.64E-06	0.0001	SWEET11
AT3G45730	-0.6426	-1.5611	1.69E-06	0.0001	AT3G45730
AT1G32520	-0.6547	-1.5743	2.19E-06	0.0001	AT1G32520
AT4G22200	-0.679	-1.601	1.88E-06	0.0001	AKT2
AT4G36040	-0.7293	-1.6579	1.81E-06	0.0001	ATJ11
AT1G67070	-0.746	-1.6772	1.83E-06	0.0001	PMI2
AT2G34490	-0.8196	-1.765	1.58E-06	0.0001	CYP710A2
AT2G38750	-0.851	-1.8037	1.73E-06	0.0001	ANN4
AT1G67600	-0.8718	-1.83	1.46E-06	0.0001	AT1G67600
AT5G45428	-0.6679	-1.5887	2.01E-06	0.0001	CPuORF24
AT1G21400	-0.6361	-1.5541	3.08E-06	0.0002	F24J8.4
AT1G11260	-0.6493	-1.5684	3.82E-06	0.0002	STP1
AT3G52720	-0.6574	-1.5773	3.11E-06	0.0002	ACA1
AT4G38420	-0.6853	-1.608	3.54E-06	0.0002	sks9
AT3G23550	-0.7098	-1.6356	2.91E-06	0.0002	LAL5
AT5G16190	-0.7255	-1.6535	3.17E-06	0.0002	CSLA11
AT1G32780	-0.7569	-1.6899	3.95E-06	0.0002	AT1G32780
AT2G21210	-0.8068	-1.7493	4.00E-06	0.0002	AT2G21210
AT3G50560	-0.807	-1.7495	3.40E-06	0.0002	AT3G50560
AT4G26260	-0.8354	-1.7844	3.88E-06	0.0002	MIOX4
AT1G23390	-0.8373	-1.7867	3.23E-06	0.0002	AT1G23390
AT4G19380	-0.8424	-1.793	2.93E-06	0.0002	FAO4A
AT4G02050	-0.7272	-1.6554	2.48E-06	0.0002	STP7
AT5G41050	-0.6098	-1.5261	4.13E-06	0.0003	AT5G41050
AT4G03960	-0.633	-1.5508	6.08E-06	0.0003	AT4G03960
AT4G21070	-0.6333	-1.5511	5.52E-06	0.0003	BRCA1
AT4G12390	-0.6455	-1.5643	4.15E-06	0.0003	PME1
AT1G01430	-0.6934	-1.617	4.11E-06	0.0003	TBL25
AT1G28670	-0.7221	-1.6495	5.02E-06	0.0003	ARAB-1
AT4G26850	-0.7741	-1.7101	4.57E-06	0.0003	VTC2
AT2G45130	-0.7834	-1.7211	5.65E-06	0.0003	SPX3
AT5G61440	-0.7997	-1.7408	5.53E-06	0.0003	ACHT5
AT3G48360	-0.8014	-1.7428	4.88E-06	0.0003	BT2
AT3G09450	-0.8279	-1.7752	4.32E-06	0.0003	AT3G09450
AT4G14680	-0.6246	-1.5418	7.06E-06	0.0004	APS3

AT1G13260	-0.6451	-1.5638	7.13E-06	0.0004	RAV1
AT4G15430	-0.6466	-1.5655	6.74E-06	0.0004	AT4G15430
AT4G38690	-0.6529	-1.5723	8.26E-06	0.0004	AT4G38690
AT3G14770	-0.6542	-1.5737	6.42E-06	0.0004	SWEET2
AT5G07690	-0.7109	-1.6368	7.74E-06	0.0004	MYB29
AT3G04070	-0.7602	-1.6938	7.08E-06	0.0004	anac047
AT5G17030	-0.8051	-1.7472	7.04E-06	0.0004	UGT78D3
AT1G79770	-0.8053	-1.7475	7.36E-06	0.0004	AT1G79770
AT2G41120	-0.5902	-1.5055	8.31E-06	0.0004	AT2G41120
AT1G80920	-0.6497	-1.5688	7.25E-06	0.0004	ATJ8
AT5G56860	-0.586	-1.5011	8.65E-06	0.0005	GATA21
AT1G24580	-0.6263	-1.5436	9.71E-06	0.0005	AT1G24580
AT5G67420	-0.6418	-1.5603	1.02E-05	0.0005	LBD37
AT2G32530	-0.679	-1.601	1.04E-05	0.0005	CSLB3
AT4G36670	-0.6911	-1.6146	8.70E-06	0.0005	PLT6
AT1G14280	-0.7212	-1.6486	9.45E-06	0.0005	PKS2
AT1G53870	-0.7769	-1.7135	1.07E-05	0.0005	AT1G53870
AT5G50790	-0.7839	-1.7218	1.04E-05	0.0005	SWEET10
AT5G35525	-0.793	-1.7327	1.06E-05	0.0005	PCR3
AT4G03510	-0.6691	-1.59	9.79E-06	0.0005	RMA1
AT1G75100	-0.5914	-1.5067	1.34E-05	0.0006	JAC1
AT2G23840	-0.609	-1.5252	1.17E-05	0.0006	AT2G23840
AT5G48485	-0.6289	-1.5464	1.27E-05	0.0006	DIR1
AT1G01180	-0.6603	-1.5805	1.20E-05	0.0006	AT1G01180
AT4G15680	-0.6805	-1.6027	1.20E-05	0.0006	GRXS4
AT4G17245	-0.707	-1.6323	1.28E-05	0.0006	AT4G17245
AT4G12470	-0.7417	-1.6722	1.17E-05	0.0006	AZI1
AT1G43800	-0.7482	-1.6796	1.27E-05	0.0006	S-ACP-DES6
AT2G22770	-0.749	-1.6806	1.29E-05	0.0006	NAI1
AT1G72890	-0.7493	-1.681	1.19E-05	0.0006	AT1G72890
AT2G17880	-0.7781	-1.7148	1.29E-05	0.0006	AT2G17880
AT1G49200	-0.7898	-1.7288	1.18E-05	0.0006	ATL75
AT3G50840	-0.6716	-1.5929	1.26E-05	0.0006	AT3G50840
AT2G30600	-0.6877	-1.6107	1.23E-05	0.0006	AT2G30600
AT1G22500	-0.7031	-1.628	1.22E-05	0.0006	ATL15
AT5G23350	-0.7623	-1.6962	1.26E-05	0.0006	AT5G23350
AT2G16380	-0.5878	-1.5029	1.40E-05	0.0007	SFH7
AT3G47750	-0.597	-1.5126	1.41E-05	0.0007	ATATH3
AT2G46450	-0.626	-1.5433	1.47E-05	0.0007	CNGC12
AT2G15890	-0.683	-1.6054	1.55E-05	0.0007	MEE14
AT3G23410	-0.5942	-1.5096	1.72E-05	0.0008	FAO3
AT1G68440	-0.6286	-1.5461	1.87E-05	0.0008	AT1G68440
AT1G03440	-0.6591	-1.5791	1.69E-05	0.0008	AT1G03440
AT1G69370	-0.6939	-1.6176	1.67E-05	0.0008	CM3
AT3G61060	-0.7499	-1.6817	1.78E-05	0.0008	PP2A13

AT1G13100	-0.6183	-1.5351	2.00E-05	0.0009	CYP71B29
AT1G62290	-0.6506	-1.5698	2.06E-05	0.0009	APA2
AT1G15580	-0.7049	-1.63	2.07E-05	0.0009	IAA5
AT5G38780	-0.71	-1.6359	2.00E-05	0.0009	AT5G38780
AT1G08310	-0.7554	-1.6881	2.05E-05	0.0009	AT1G08310
AT3G10150	-0.7603	-1.6939	2.03E-05	0.0009	PAP16
AT5G17860	-0.6125	-1.5289	2.42E-05	0.001	CCX1
AT3G21010	-0.758	-1.6912	2.46E-05	0.001	AT3G21010
AT4G38860	-0.7626	-1.6966	2.40E-05	0.001	AT4G38860

Up-regulated genes iaa5,6,19 vs Col-0 during stress (FDR < 0.001

GeneID	Genotype =>	Genotype =>	Genotype => iaa5	Genotype => iaa561	GeneName
AT4G08093	1.7298	3.3168	2.91E-24	1.53E-20	AT4G08093
AT4G31940	1.7008	3.2508	2.13E-21	8.01E-18	CYP82C4
AT3G03341	1.2225	2.3335	6.35E-16	8.82E-13	AT3G03341
AT1G11080	1.0681	2.0967	2.00E-15	2.63E-12	SCPL31
AT3G62270	0.803	1.7447	3.91E-15	4.54E-12	BOR2
AT1G07430	1.0524	2.074	1.57E-14	1.30E-11	AIP1
AT5G56080	1.3521	2.5528	2.76E-14	2.02E-11	NAS2
AT2G28780	1.0299	2.0418	4.69E-14	3.02E-11	AT2G28780
AT1G20030	0.9097	1.8787	4.87E-14	3.06E-11	AT1G20030
AT2G39800	0.9305	1.9059	8.32E-14	4.99E-11	P5CSA
AT1G01580	1.3174	2.4922	9.26E-14	5.31E-11	FRO2
AT3G02550	1.1501	2.2193	1.85E-13	9.41E-11	LBD41
AT3G27150	1.1158	2.1671	3.41E-13	1.60E-10	AT3G27150
AT1G30510	0.7679	1.7028	5.31E-13	2.37E-10	RFNR2
AT1G49860	1.0054	2.0075	1.06E-12	4.22E-10	GSTF14
AT3G12900	1.2446	2.3696	2.75E-12	1.02E-09	AT3G12900
AT5G02780	1.1309	2.1899	1.40E-11	4.79E-09	GSTL1
AT1G69880	1.0113	2.0157	1.79E-11	5.90E-09	TRX8
AT3G43190	0.915	1.8856	4.09E-11	1.26E-08	SUS4
AT3G13784	1.0575	2.0813	1.39E-10	3.71E-08	AtcwINV5
AT2G39510	0.8018	1.7432	2.11E-10	5.52E-08	AT2G39510
AT3G63060	0.7347	1.6641	2.79E-10	6.94E-08	EDL3
AT4G17350	0.8961	1.8611	2.99E-10	7.38E-08	AT4G17350
AT3G01260	0.8552	1.809	5.86E-10	1.31E-07	AT3G01260
AT5G14650	0.9594	1.9445	8.87E-10	1.90E-07	AT5G14650
AT2G41190	0.7563	1.6892	2.26E-09	4.26E-07	AT2G41190
AT3G62040	0.7693	1.7044	3.26E-09	5.74E-07	AT3G62040
AT5G66460	0.6575	1.5774	4.44E-09	7.27E-07	MAN7
AT5G15120	0.9821	1.9753	5.28E-09	8.44E-07	PCO1
AT2G18980	0.9526	1.9353	5.27E-09	8.44E-07	PER16
AT4G02290	0.6307	1.5484	5.61E-09	8.92E-07	AtGH9B13
AT5G66400	0.9933	1.9907	6.32E-09	9.87E-07	RAB18
AT3G28510	1.0331	2.0464	7.16E-09	1.10E-06	AT3G28510

AT1G51830	0.7281	1.6564	7.26E-09	1.11E-06	AT1G51830
AT1G52040	1.0259	2.0362	1.45E-08	1.98E-06	MBP1
AT3G46270	1.0055	2.0076	2.67E-08	3.35E-06	AT3G46270
AT1G02205	0.8763	1.8357	2.95E-08	3.64E-06	CER1
AT2G26150	0.8859	1.8479	3.08E-08	3.77E-06	HSFA2
AT2G43570	0.9237	1.897	3.38E-08	4.00E-06	CHI
AT3G58810	0.9031	1.8701	4.64E-08	5.30E-06	MTPA2
AT1G60190	0.6567	1.5765	5.30E-08	6.01E-06	PUB19
AT1G32450	0.7334	1.6625	5.77E-08	6.47E-06	NPF7.3
AT4G24310	0.9726	1.9623	6.58E-08	7.23E-06	AT4G24310
AT5G01520	0.7678	1.7027	7.54E-08	8.16E-06	AT5G01520
AT1G47600	0.9195	1.8914	7.76E-08	8.32E-06	TGG4
AT4G08570	0.9695	1.9581	7.87E-08	8.41E-06	AT4G08570
AT1G01240	0.6685	1.5894	1.01E-07	1.06E-05	AT1G01240
AT3G04620	0.9161	1.887	1.10E-07	1.14E-05	AT3G04620
AT5G57050	0.7404	1.6707	1.22E-07	1.24E-05	ABI2
AT2G40130	0.7644	1.6986	1.27E-07	1.28E-05	AT2G40130
AT5G41610	0.6186	1.5354	2.05E-07	1.95E-05	CHX18
AT1G01360	0.6848	1.6075	2.10E-07	1.99E-05	PYL9
AT1G14080	0.8573	1.8116	2.16E-07	2.03E-05	FUT6
AT5G15500	0.9326	1.9087	2.58E-07	2.38E-05	AT5G15500
AT1G78990	0.7465	1.6777	3.13E-07	2.82E-05	AT1G78990
AT5G63350	0.902	1.8687	3.18E-07	2.86E-05	AT5G63350
AT4G22990	0.7189	1.6459	3.26E-07	2.89E-05	AT4G22990
AT4G23060	0.6805	1.6027	3.39E-07	2.98E-05	IQD22
AT1G49570	0.8946	1.8591	3.93E-07	3.39E-05	PER10
AT3G05650	0.842	1.7925	4.57E-07	3.86E-05	AtRLP32
AT1G68880	0.7838	1.7217	5.29E-07	4.34E-05	AtbZIP
AT1G44970	0.7073	1.6328	5.29E-07	4.34E-05	PER9
AT2G36270	0.7808	1.718	6.14E-07	5.03E-05	ABI5
AT3G61270	0.7195	1.6466	6.83E-07	5.44E-05	AT3G61270
AT4G35560	0.7296	1.6581	7.65E-07	6.05E-05	AT4G35560
AT4G01970	0.8342	1.7829	7.84E-07	6.14E-05	RFS4
AT1G19960	0.7848	1.7229	8.25E-07	6.44E-05	AT1G19960
AT2G18370	0.7368	1.6665	1.04E-06	7.97E-05	LTP8
AT2G47780	0.8182	1.7632	1.09E-06	8.24E-05	AT2G47780
AT5G54165	0.8639	1.82	1.11E-06	8.36E-05	AT5G54165
AT1G06080	0.7368	1.6665	1.14E-06	8.52E-05	ADS1
AT2G33380	0.841	1.7913	1.30E-06	9.44E-05	PXG3
AT5G05220	0.8333	1.7817	1.33E-06	9.61E-05	AT5G05220
AT4G12520	0.8216	1.7674	1.63E-06	0.0001	AT4G12520
AT2G40750	0.7568	1.6897	1.40E-06	0.0001	WRKY54
AT2G21130	0.6364	1.5545	1.55E-06	0.0001	CYP19-2
AT4G21930	0.8312	1.7792	1.81E-06	0.0001	AT4G21930
AT3G14360	0.6279	1.5453	2.16E-06	0.0001	AT3G14360

AT2G17036	0.7962	1.7365	3.31E-06	0.0002	AT2G17036
AT3G04570	0.7121	1.6381	3.49E-06	0.0002	AHL19
ATCG00490	0.6219	1.5389	3.99E-06	0.0002	RBCL
AT5G47060	0.5907	1.506	3.60E-06	0.0002	AT5G47060
AT3G22100	0.7904	1.7296	5.00E-06	0.0003	BHLH117
AT2G25810	0.6979	1.6221	6.15E-06	0.0003	TIP4-1
AT1G77330	0.6336	1.5514	4.87E-06	0.0003	AT1G77330
AT1G56320	0.7337	1.6629	4.86E-06	0.0003	AT1G56320
AT5G47640	0.6885	1.6116	5.58E-06	0.0003	NFYB2
AT5G01870	0.7845	1.7225	6.28E-06	0.0004	LTP10
AT3G04630	0.6381	1.5563	8.18E-06	0.0004	WDL1
AT5G47635	0.8068	1.7493	6.25E-06	0.0004	AT5G47635
AT5G53320	0.6092	1.5255	7.29E-06	0.0004	AT5G53320
AT2G37700	0.7979	1.7386	1.04E-05	0.0005	AT2G37700
AT5G44420	0.7801	1.7172	8.70E-06	0.0005	PDF1.2A
AT2G41070	0.6322	1.55	1.06E-05	0.0005	DPBF4
AT2G39530	0.7787	1.7156	1.20E-05	0.0006	AT2G39530
AT4G31910	0.7453	1.6763	1.18E-05	0.0006	AT4G31910
AT4G31320	0.7146	1.641	1.24E-05	0.0006	AT4G31320
AT3G63430	0.594	1.5095	1.33E-05	0.0006	AT3G63430
AT3G62280	0.7282	1.6566	1.57E-05	0.0007	AT3G62280
AT1G08430	0.7231	1.6508	1.58E-05	0.0007	ALMT1
AT3G05640	0.7147	1.6411	1.60E-05	0.0007	AT3G05640
AT2G37180	0.6938	1.6176	1.48E-05	0.0007	PIP2-3
AT2G19810	0.6416	1.5601	1.55E-05	0.0007	AT2G19810
AT3G11410	0.6123	1.5286	1.63E-05	0.0007	PP2CA
AT3G62090	0.5964	1.5119	1.59E-05	0.0007	PIF6
AT5G57090	0.7228	1.6503	1.69E-05	0.0008	PIN2
AT5G58160	0.613	1.5294	1.89E-05	0.0008	AT5G58160
AT3G58550	0.726	1.6541	1.90E-05	0.0008	AT3G58550
AT5G10580	0.6768	1.5986	1.69E-05	0.0008	AT5G10580
AT5G05840	0.7716	1.7071	1.94E-05	0.0009	AT5G05840
AT3G06160	0.75	1.6818	2.04E-05	0.0009	REM21
AT3G49860	0.6658	1.5864	1.96E-05	0.0009	ATARLA1B
AT1G31880	0.5875	1.5027	2.34E-05	0.001	BRX
AT1G13590	0.7624	1.6963	2.49E-05	0.0011	PSK1
AT4G22810	0.7449	1.6758	2.75E-05	0.0011	AHL24
AT2G47770	0.7379	1.6677	2.80E-05	0.0011	TSPO
AT3G16440	0.7183	1.6452	2.54E-05	0.0011	JAL32
AT2G02120	0.6832	1.6057	2.60E-05	0.0011	PDF2.1
AT4G38400	0.5889	1.5041	2.73E-05	0.0011	EXLA2
AT1G01570	0.6648	1.5854	2.99E-05	0.0012	AT1G01570
AT3G45160	0.6138	1.5302	3.03E-05	0.0012	AT3G45160
AT2G18150	0.5901	1.5053	2.99E-05	0.0012	PER15
AT5G63660	0.736	1.6656	3.90E-05	0.0015	PDF2.5

AT1G53270	0.665	1.5856	3.84E-05	0.0015	ABCG10
AT1G53170	0.6604	1.5806	4.00E-05	0.0015	ERF8
AT3G21330	0.732	1.6609	4.23E-05	0.0016	BHLH87
AT1G50060	0.7289	1.6574	4.35E-05	0.0016	AT1G50060
AT5G60530	0.7365	1.6662	4.50E-05	0.0017	AT5G60530
AT3G07970	0.7242	1.652	4.41E-05	0.0017	QRT2
AT3G53160	0.6217	1.5387	4.74E-05	0.0017	UGT73C7
AT5G53710	0.7219	1.6494	4.85E-05	0.0018	AT5G53710
AT1G56600	0.709	1.6347	5.00E-05	0.0018	GOLS2
AT3G56275	0.7291	1.6576	5.47E-05	0.002	AT3G56275
AT5G45070	0.7217	1.6492	5.62E-05	0.002	PP2A8
AT2G35950	0.713	1.6393	5.75E-05	0.002	EDA12
AT5G07475	0.6263	1.5436	5.66E-05	0.002	AT5G07475
AT5G10210	0.6812	1.6034	5.65E-05	0.002	AT5G10210
AT1G02180	0.6074	1.5235	5.68E-05	0.002	AT1G02180
AT3G21890	0.6452	1.564	5.88E-05	0.0021	AT3G21890
AT3G27250	0.7242	1.652	6.30E-05	0.0022	AT3G27250
AT5G54370	0.7209	1.6482	6.80E-05	0.0023	AT5G54370
AT4G10510	0.7166	1.6433	6.93E-05	0.0024	AT4G10510
AT2G42530	0.6902	1.6135	7.10E-05	0.0024	COR15B
AT5G47920	0.6209	1.5378	7.20E-05	0.0024	AT5G47920
AT5G15130	0.708	1.6336	7.53E-05	0.0025	WRKY72
AT5G62340	0.6803	1.6025	7.38E-05	0.0025	AT5G62340
AT1G61260	0.6659	1.5865	8.23E-05	0.0027	AT1G61260
AT1G75060	0.6154	1.532	8.14E-05	0.0027	AT1G75060
AT5G28370	0.711	1.6369	8.58E-05	0.0028	AT5G28370
AT1G80240	0.6449	1.5637	9.10E-05	0.0029	AT1G80240
AT1G01030	0.6287	1.5461	0.0001	0.0033	NGA3
AT1G66950	0.696	1.62	0.0001	0.0034	ABCG39
AT5G66280	0.647	1.5659	0.0001	0.0038	GMD1
AT5G02020	0.6814	1.6036	0.0001	0.0039	SIS
AT2G48080	0.5984	1.5141	0.0001	0.0039	AT2G48080
AT4G19690	0.6661	1.5868	0.0001	0.004	IRT1
AT4G25692	0.6214	1.5384	0.0002	0.0044	CPuORF13
AT5G45080	0.6833	1.6058	0.0002	0.0046	PP2A6
AT2G45430	0.6448	1.5635	0.0002	0.0046	AHL22
AT2G37210	0.6381	1.5563	0.0002	0.0046	LOG3
AT2G24720	0.6051	1.5211	0.0002	0.0046	GLR2.2
AT3G13020	0.594	1.5095	0.0002	0.0046	AT3G13020
AT3G23175	0.5987	1.5144	0.0002	0.0048	AT3G23175
AT5G13870	0.5881	1.5033	0.0002	0.0048	XTH5
AT5G60520	0.6725	1.5938	0.0002	0.0053	AT5G60520
AT4G39340	0.6664	1.5871	0.0002	0.0055	EC1.4
AT3G53235	0.6709	1.592	0.0002	0.0056	AT3G53235
AT1G72870	0.6645	1.585	0.0002	0.0057	AT1G72870

AT2G23630	0.6664	1.5871	0.0002	0.0059	sks16
AT1G68150	0.6281	1.5456	0.0002	0.0059	WRKY9
AT5G24080	0.6315	1.5492	0.0002	0.0062	AT5G24080
AT1G72360	0.6349	1.5528	0.0003	0.0064	ERF073
AT2G32620	0.637	1.5551	0.0003	0.0066	CSLB2
AT3G25190	0.6057	1.5217	0.0003	0.0068	AT3G25190
AT4G03540	0.6572	1.577	0.0003	0.0069	AT4G03540
AT5G57123	0.6543	1.5739	0.0003	0.007	AT5G57123
AT4G28140	0.6433	1.5619	0.0003	0.007	ERF054
AT1G67330	0.5928	1.5081	0.0003	0.0074	AT1G67330
AT2G28160	0.6438	1.5624	0.0003	0.0075	FIT
AT1G21340	0.6164	1.533	0.0003	0.0076	DOF1.2
AT5G13990	0.65	1.5692	0.0003	0.0078	ATEXO70C2
AT1G51470	0.6419	1.5604	0.0003	0.0079	TGG5
AT3G10040	0.5976	1.5132	0.0003	0.008	AT3G10040
AT2G20880	0.6384	1.5566	0.0004	0.0083	ERF053
AT5G50760	0.6264	1.5437	0.0004	0.0089	AT5G50760
AT5G17540	0.6404	1.5588	0.0004	0.0089	AT5G17540
AT1G62280	0.5963	1.5118	0.0004	0.0092	SLAH1
AT4G33467	0.6101	1.5264	0.0004	0.0095	AT4G33467
AT1G56680	0.637	1.5551	0.0004	0.0096	AT1G56680
AT3G15240	0.6289	1.5464	0.0004	0.0096	AT3G15240
AT3G61930	0.6224	1.5394	0.0004	0.0098	AT3G61930
AT1G10810	0.6104	1.5267	0.0005	0.0099	AT1G10810
AT1G07550	0.6244	1.5416	0.0005	0.01	AT1G07550
AT3G24300	0.5919	1.5073	0.0005	0.01	AMT1-3
AT4G21930	0.8312	1.7792	1.81E-06	0.0001	AT4G21930
AT3G14360	0.6279	1.5453	2.16E-06	0.0001	AT3G14360
AT2G17036	0.7962	1.7365	3.31E-06	0.0002	AT2G17036
AT3G04570	0.7121	1.6381	3.49E-06	0.0002	AHL19
ATCG00490	0.6219	1.5389	3.99E-06	0.0002	RBCL
AT5G47060	0.5907	1.506	3.60E-06	0.0002	AT5G47060
AT3G22100	0.7904	1.7296	5.00E-06	0.0003	BHLH117
AT2G25810	0.6979	1.6221	6.15E-06	0.0003	TIP4-1
AT1G77330	0.6336	1.5514	4.87E-06	0.0003	AT1G77330
AT1G56320	0.7337	1.6629	4.86E-06	0.0003	AT1G56320
AT5G47640	0.6885	1.6116	5.58E-06	0.0003	NFYB2
AT5G01870	0.7845	1.7225	6.28E-06	0.0004	LTP10
AT3G04630	0.6381	1.5563	8.18E-06	0.0004	WDL1
AT5G47635	0.8068	1.7493	6.25E-06	0.0004	AT5G47635
AT5G53320	0.6092	1.5255	7.29E-06	0.0004	AT5G53320
AT2G37700	0.7979	1.7386	1.04E-05	0.0005	AT2G37700
AT5G44420	0.7801	1.7172	8.70E-06	0.0005	PDF1.2A
AT2G41070	0.6322	1.55	1.06E-05	0.0005	DPBF4
AT2G39530	0.7787	1.7156	1.20E-05	0.0006	AT2G39530

AT4G31910	0.7453	1.6763	1.18E-05	0.0006	AT4G31910
AT4G31320	0.7146	1.641	1.24E-05	0.0006	AT4G31320
AT3G63430	0.594	1.5095	1.33E-05	0.0006	AT3G63430
AT3G62280	0.7282	1.6566	1.57E-05	0.0007	AT3G62280
AT1G08430	0.7231	1.6508	1.58E-05	0.0007	ALMT1
AT3G05640	0.7147	1.6411	1.60E-05	0.0007	AT3G05640
AT2G37180	0.6938	1.6176	1.48E-05	0.0007	PIP2-3
AT2G19810	0.6416	1.5601	1.55E-05	0.0007	AT2G19810
AT3G11410	0.6123	1.5286	1.63E-05	0.0007	PP2CA
AT3G62090	0.5964	1.5119	1.59E-05	0.0007	PIF6
AT5G57090	0.7228	1.6503	1.69E-05	0.0008	PIN2
AT5G58160	0.613	1.5294	1.89E-05	0.0008	AT5G58160
AT3G58550	0.726	1.6541	1.90E-05	0.0008	AT3G58550
AT5G10580	0.6768	1.5986	1.69E-05	0.0008	AT5G10580
AT5G05840	0.7716	1.7071	1.94E-05	0.0009	AT5G05840
AT3G06160	0.75	1.6818	2.04E-05	0.0009	REM21
AT3G49860	0.6658	1.5864	1.96E-05	0.0009	ATARLA1B
AT1G31880	0.5875	1.5027	2.34E-05	0.001	BRX
AT1G13590	0.7624	1.6963	2.49E-05	0.0011	PSK1
AT4G22810	0.7449	1.6758	2.75E-05	0.0011	AHL24
AT2G47770	0.7379	1.6677	2.80E-05	0.0011	TSPO
AT3G16440	0.7183	1.6452	2.54E-05	0.0011	JAL32
AT2G02120	0.6832	1.6057	2.60E-05	0.0011	PDF2.1
AT4G38400	0.5889	1.5041	2.73E-05	0.0011	EXLA2
AT1G01570	0.6648	1.5854	2.99E-05	0.0012	AT1G01570
AT3G45160	0.6138	1.5302	3.03E-05	0.0012	AT3G45160
AT2G18150	0.5901	1.5053	2.99E-05	0.0012	PER15
AT5G63660	0.736	1.6656	3.90E-05	0.0015	PDF2.5
AT1G53270	0.665	1.5856	3.84E-05	0.0015	ABCG10
AT1G53170	0.6604	1.5806	4.00E-05	0.0015	ERF8
AT3G21330	0.732	1.6609	4.23E-05	0.0016	BHLH87
AT1G50060	0.7289	1.6574	4.35E-05	0.0016	AT1G50060
AT5G60530	0.7365	1.6662	4.50E-05	0.0017	AT5G60530
AT3G07970	0.7242	1.652	4.41E-05	0.0017	QRT2
AT3G53160	0.6217	1.5387	4.74E-05	0.0017	UGT73C7
AT5G53710	0.7219	1.6494	4.85E-05	0.0018	AT5G53710
AT1G56600	0.709	1.6347	5.00E-05	0.0018	GOLS2
AT3G56275	0.7291	1.6576	5.47E-05	0.002	AT3G56275
AT5G45070	0.7217	1.6492	5.62E-05	0.002	PP2A8
AT2G35950	0.713	1.6393	5.75E-05	0.002	EDA12
AT5G07475	0.6263	1.5436	5.66E-05	0.002	AT5G07475
AT5G10210	0.6812	1.6034	5.65E-05	0.002	AT5G10210
AT1G02180	0.6074	1.5235	5.68E-05	0.002	AT1G02180
AT3G21890	0.6452	1.564	5.88E-05	0.0021	AT3G21890
AT3G27250	0.7242	1.652	6.30E-05	0.0022	AT3G27250

AT5G54370	0.7209	1.6482	6.80E-05	0.0023	AT5G54370
AT4G10510	0.7166	1.6433	6.93E-05	0.0024	AT4G10510
AT2G42530	0.6902	1.6135	7.10E-05	0.0024	COR15B
AT5G47920	0.6209	1.5378	7.20E-05	0.0024	AT5G47920
AT5G15130	0.708	1.6336	7.53E-05	0.0025	WRKY72
AT5G62340	0.6803	1.6025	7.38E-05	0.0025	AT5G62340
AT1G61260	0.6659	1.5865	8.23E-05	0.0027	AT1G61260
AT1G75060	0.6154	1.532	8.14E-05	0.0027	AT1G75060
AT5G28370	0.711	1.6369	8.58E-05	0.0028	AT5G28370
AT1G80240	0.6449	1.5637	9.10E-05	0.0029	AT1G80240
AT1G01030	0.6287	1.5461	0.0001	0.0033	NGA3
AT1G66950	0.696	1.62	0.0001	0.0034	ABCG39
AT5G66280	0.647	1.5659	0.0001	0.0038	GMD1
AT5G02020	0.6814	1.6036	0.0001	0.0039	SIS
AT2G48080	0.5984	1.5141	0.0001	0.0039	AT2G48080
AT4G19690	0.6661	1.5868	0.0001	0.004	IRT1
AT4G25692	0.6214	1.5384	0.0002	0.0044	CPuORF13
AT5G45080	0.6833	1.6058	0.0002	0.0046	PP2A6
AT2G45430	0.6448	1.5635	0.0002	0.0046	AHL22
AT2G37210	0.6381	1.5563	0.0002	0.0046	LOG3
AT2G24720	0.6051	1.5211	0.0002	0.0046	GLR2.2
AT3G13020	0.594	1.5095	0.0002	0.0046	AT3G13020
AT3G23175	0.5987	1.5144	0.0002	0.0048	AT3G23175
AT5G13870	0.5881	1.5033	0.0002	0.0048	XTH5
AT5G60520	0.6725	1.5938	0.0002	0.0053	AT5G60520
AT4G39340	0.6664	1.5871	0.0002	0.0055	EC1.4
AT3G53235	0.6709	1.592	0.0002	0.0056	AT3G53235
AT1G72870	0.6645	1.585	0.0002	0.0057	AT1G72870
AT2G23630	0.6664	1.5871	0.0002	0.0059	sks16
AT1G68150	0.6281	1.5456	0.0002	0.0059	WRKY9
AT5G24080	0.6315	1.5492	0.0002	0.0062	AT5G24080
AT1G72360	0.6349	1.5528	0.0003	0.0064	ERF073
AT2G32620	0.637	1.5551	0.0003	0.0066	CSLB2
AT3G25190	0.6057	1.5217	0.0003	0.0068	AT3G25190
AT4G03540	0.6572	1.577	0.0003	0.0069	AT4G03540
AT5G57123	0.6543	1.5739	0.0003	0.007	AT5G57123
AT4G28140	0.6433	1.5619	0.0003	0.007	ERF054
AT1G67330	0.5928	1.5081	0.0003	0.0074	AT1G67330
AT2G28160	0.6438	1.5624	0.0003	0.0075	FIT
AT1G21340	0.6164	1.533	0.0003	0.0076	DOF1.2
AT5G13990	0.65	1.5692	0.0003	0.0078	ATEXO70C2
AT1G51470	0.6419	1.5604	0.0003	0.0079	TGG5
AT3G10040	0.5976	1.5132	0.0003	0.008	AT3G10040
AT2G20880	0.6384	1.5566	0.0004	0.0083	ERF053
AT5G50760	0.6264	1.5437	0.0004	0.0089	AT5G50760

AT5G17540	0.6404	1.5588	0.0004	0.0089	AT5G17540
AT1G62280	0.5963	1.5118	0.0004	0.0092	SLAH1
AT4G33467	0.6101	1.5264	0.0004	0.0095	AT4G33467
AT1G56680	0.637	1.5551	0.0004	0.0096	AT1G56680
AT3G15240	0.6289	1.5464	0.0004	0.0096	AT3G15240
AT3G61930	0.6224	1.5394	0.0004	0.0098	AT3G61930
AT1G10810	0.6104	1.5267	0.0005	0.0099	AT1G10810
AT1G07550	0.6244	1.5416	0.0005	0.01	AT1G07550
AT3G24300	0.5919	1.5073	0.0005	0.01	AMT1-3
AT1G52060	0.6312	1.5489	0.0005	0.0101	JAL9
AT2G30340	0.6302	1.5478	0.0005	0.0101	LBD13
AT5G52300	0.6161	1.5327	0.0005	0.0101	LTI65
AT1G34844	0.6327	1.5504	0.0005	0.0101	AT1G34844
AT5G40000	0.6225	1.5395	0.0005	0.0104	AT5G40000
AT5G50360	0.586	1.5011	0.0005	0.0105	AT5G50360
AT5G53390	0.6146	1.5311	0.0005	0.0112	AT5G53390
AT1G68430	0.5903	1.5056	0.0006	0.0114	AT1G68430
AT2G35600	0.5956	1.5111	0.0006	0.0119	BRXL1
ATMG01360	0.6191	1.5359	0.0006	0.0124	COX1
AT5G48940	0.6033	1.5192	0.0007	0.0129	RCH1
AT2G34850	0.6006	1.5164	0.0008	0.0152	MEE25
AT5G04970	0.6014	1.5171	0.0009	0.0158	PME47
AT3G52160	0.5999	1.5156	0.0009	0.0158	KCS15
AT3G55150	0.5926	1.5079	0.001	0.0171	ATEXO70H1
AT2G31920	0.5896	1.5049	0.0011	0.0188	AT2G31920
AT3G54770	0.5897	1.5049	0.0011	0.019	ARP1
AT3G49190	0.587	1.5021	0.0012	0.0202	AT3G49190

Table S2-Indolic and aliphatic glucosinolate levels as measured by HPLC in the Col-0 and *iaa5,6,19* mutants over a period of 3 hours. Each value is the mean +/- SE (nmol/mgFW)

Indolic GLS	**Indol-3-ylmethyl glucosinolate (I3M)**			
	0 min	30 min	60 min	180 min
Col-0	0.0020 +/-0.002	0.0028 +/-0.002	0.0022 +/-0.002	0.0023 +/-0.002
iaa5,6,19	0.0043 +/-0.004	0.0029 +/-0.002	0.0016 +/-0.001	0.0026 +/-0.002
	4-methylthioalkyl glucosinolate (4-MT)			
Col-0	0.0195 +/-0.001	0.0115 +/-0.000	0.0100 +/-0.000	0.0078 +/-0.000
iaa5,6,19	0.0160 +/-0.001	0.0131 +/-0.001	0.0106 +/-0.000	0.0112 +/-0.000
	***N*-methoxy-indol-3-ylmethyl glucosinolate (4NMIOM)**			
Col-0	0.1021 +/-0.003	0.0833 +/-0.006	0.1025 +/-0.003	0.0820 +/-0.009
iaa5,6,19	0.088 +/-0.005	0.0656 +/-0.005	0.0727 +/-0.006	0.0726 +/-0.003
	8-methylthioalkyl glucosinolate (8-MT)			
Col-0	0.0845 +/-0.019	0.0727 +/-0.021	0.0686 +/-0.020	0.0451 +/-0.016
iaa5,6,19	0.0891 +/-0.038	0.0592 +/-0.019	0.0588 +/-0.017	0.0535 +/-0.023
Aliphatic GLS	**3-Methylsulfinylpropyl glucosinolate (3-MSO)**			
Col-0	0.0329 +/-0.004	0.0337 +/-0.001	0.0296 +/-0.006	0.0246 +/-0.005
iaa5,6,19	0.0354 +/-0.003	0.0123 +/-0.003	0.0185 +/-0.005	0.0143 +/-0.004
	4-Methylsulfinylbutyl glucosinolate (4-MSO)			
Col-0	0.2287 +/-0.032	0.2080 +/-0.030	0.2511 +/-0.018	0.2517 +/-0.021
iaa5,6,19	0.2460 +/-0.030	0.1767 +/-0.016	0.2022 +/-0.018	0.2005 +/-0.025
	5-Methylsulfinylpentyl glucosinolate (5-MSO)			
Col-0	0.0155 +/-0.000	0.0126 +/-0.000	0.0148 +/-0.001	0.0142 +/-0.001
iaa5,6,19	0.0147 +/-0.001	0.0141 +/-0.001	0.0121 +/-0.001	0.0134 +/-0.002
	7-Methylsulfinylheptyl glucosinolate (7-MSO)			
Col-0	0.0130 +/-0.000	0.0119 +/-0.000	0.0127 +/-0.001	0.0112 +/-0.001
iaa5,6,19	0.0150 +/-0.000	0.0123 +/-0.000	0.0141 +/-0.001	0.0166 +/-0.001
	8-methylsulfinyloctyl glucosinolate (8-MSO)			
Col-0	0.0461 +/-0.009	0.0396 +/-0.006	0.0467 +/-0.011	0.0390 +/-0.012
iaa5,6,19	0.0463 +/-0.013	0.0335 +/-0.005	0.0375 +/-0.012	0.0407 +/-0.009

Table S3. Primers used in this stidy

qPCR

Primer Numb	Primer Name	Primer Sequence, 5'-3'	Primer Purpose
MS433	qMYB29 F	CGTTGATTGCTTACCGGACT	qPCR of MYB29
MS434	qMYB29 R	AGTGACCCTATAGTGGACCTTTACT	Do
MS435	qCYP79F1 F	CTTGACGTACTGTCGTTTGTTG	qPCR of CYP79F1
MS436	qCYP79F1 R	GCTACTCCGAATGTTTGATCG	Do
MS437	qCYP79F2 F	TGATGTGTTTCGACGCTTTG	qPCR of CYP79F2
MS438	qCYP79F2 R	TATAGCGTTTTCGGGCAATG	Do
MS439	qCYP83A1 F	TGGCAATCGTCTCTCTATCTTTC	qPCR of CYP83A1
MS440	qCYP83A1 R	GACATCATGTGAATTTGCTTCC	Do
MS441	qSUR2 F	CCATCAAATTCACTCACGAAAATGTC	qPCR of CYP8B1/SUR2
MS442	qSUR2 R	AAGGTAAGTCATGGCCCATACCACC	Do
MS443	qSUR1 F	CCGGCAAAGGCAATTCTTACGG	qPCR of SUR1
MS444	qSUR1 R	TCATATAATCAGCAACGGCTCGTC	Do
MS445	qMYB28 F	AGACTGCGATGGACCAACTACC	qPCR of MYB28
MS446	qMYB28 R	TCTCGCTATGACCGACCACTTG	Do
MS451	qWRKY63 F	AACATCGATCACAAGGCTGTGG	qPCR of WRKY63
MS452	qWRKY63 R	TCTTGAGGATGTTAGCGCATCCC	Do

Genotyping and cloning

MS446	qMYB28 R	TCTCGCTATGACCGACCACTTG	Genotyping MYB28 OE
MS457	genoMYB29 1R	TCATATGAAGTTCTTGTCGTCGT	Genotyping MYB29 OE
	35S F	GGGATGACGCACAATCCCACTATC	Genotyping 35Spromoter in MYB28 and MYB29 OE
MS459	cWRKY63_F	CACCTAATATGTTGCTCAACTTTCATAGGAC	For cloning of WRKY63 promoter +genomic DNA without STOP codon into pENTR/D/GW.
MS460	cWRKY63_R	AAACAACATCAGGTCTTCCGA	Do
MS461	sWRKY63_1F	ATTGAAGTTTCCACGCTAT	Sequencing WRKY63
MS462	sWRKY63_2F	CGAGACATGGCAGGTCTTGT	Do
MS463	sWRKY63_3F	CCTTTGGGGTGCATGATAATACG	Do
MS464	sWRKY63_1R	GTTGTCGAGGACCGTCTTGA	Do
MS465	sWRKY63_2R	GCATAGCAGTTTTGGTCTTTTGC	Do
MS466	sWRKY63_3R	ACAACATCAGGTCTTCCGATGA	Do
MS468	cIAA19g_2F	GGACGTGGGAACATGCTTGTAGT	Cloning IAA19pro-IAA19g in pCR8-GW-TOPO
MS425	cIAA19g_R	ACTCAACACTCAAGAAACAAGTAGTGT	Do
MS469	sIAA19_F	TCTCTCATGTGACCGACCAC	Sequencing IAA19
MS470	sIAA19_1R	GCGAGCATCCAGTCTCCATC	Do
MS471	sIAA19_2R	TCAACACTCAAGAAACAAGTAGTGT	Do
MS474	cIAA19_NcoI F	GCCCCATGGATGGAGAAGGAAGGACTCGG	Cloning IAA19 genomic with 3'UTR in pGREENII-0179-GC1p binary
MS475	cIAA19_BsaBI R	GCCGATACGCATCACTCAACACTCAAGAAACAAGTAGTGT	Do
MS476	cDREB2A_NcoI F	GCCCCATGGATGGCAGTTTATGATCAGAGTGGA	Cloning DREB2A CDs in pGREENII-0179-GC1p binary
MS477	cDREB2A_BsaBI R	GCCGATACGCATCTTAGTTCTCCAGATCCAAGTAACTCA	Do
MS478	GC1 F seq primer	TGTGATCTCTATCCAACA	Sequencing DREB2A CDs fusion with GC1 Promoter
MS479	nosT R seq primer	AACGTCATGCATTACATG	Sequencing presence of nosT
MS493	qMAM3_F	CGCCATTCATTGTCATAACG	
MS494	qMAM3_R	CATCACGACCTCTTCAAGC	
MS495	qSOT18_F	CCTCATCTCCACGTTTCCTC	
MS496	qSOT18_R	CATACTCGATCAGGGGCTCT	
MS497	qUGT74B1_F	CGTTTCGTATCCGTGGCTTA	
MS498	qUGT74B1_RCAGACTCACCATTTTCACAATCT		

ChIP qPCR

MS481	MYB29 q1R	ATAAGCCTGGCACTCGTGTAG	ChIP around W box in MYB29 promoter
MS484	MYB29 q3F	GTCACTAACACTCACTCTTGATG	Do
MS487	MYB28 q2F	GTCAAGAAAGCCATGTTGCG	ChIP around W box in MYB28 promoter
MS488	MYB28 q2R	CACCGTTTCAACCCTAATCAG	
MS489	WRKY63_ChIP_q1F	CTAAATCCTCTCATAGTCTCATC	ChIP around AuxRE in IAA19 promoter
MS490	WRKY63_ChIP_q1R	TCCAGATCCTTTCCCACTTCG	Do
MS491	WRKY63_ChIP_q2F	GAGAAGAAGACAAGTCTACTTTT	Do
MS492	WRKY63_ChIP_q2R	CGAAGAACATCGGCCATGAT	Do

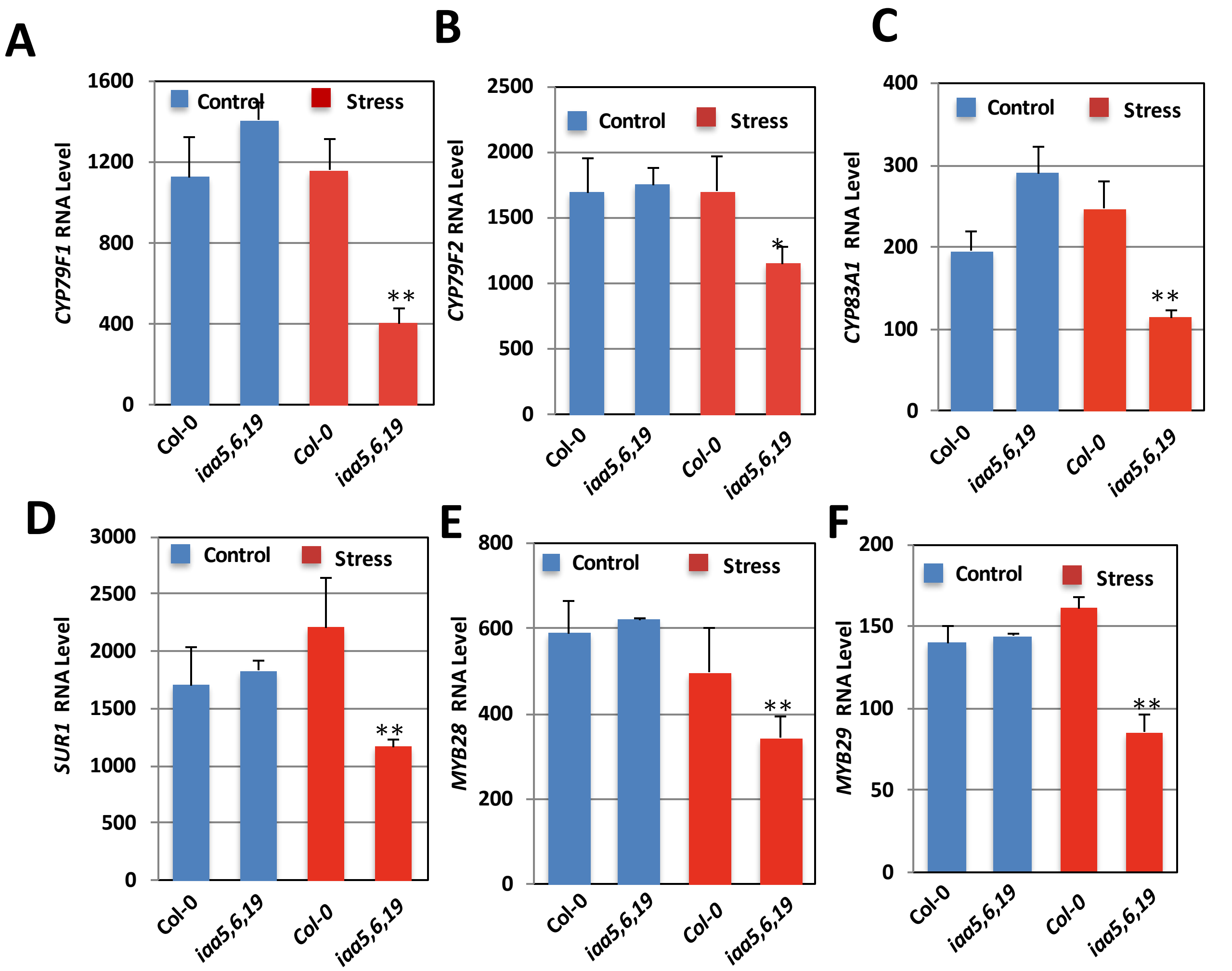

Supplementary Figure S1. **Aliphatic glucosinolate biosynthesis genes are downregulated in the *iaa5,6,19* mutant during dehydration stress.** **(A)** qRT PCR data showing actual RNA values of *CYP79F1*. **(B)** *CYP79F2*, **(C)** *CYP83A1*, **(D)** *SUR1*, **(E)** *MYB28*, **(F)** *MYB29*. For panels differences between the mutant and corresponding Col-0 control are significant at $p < 0.05$ (*) and $p < 0.01$ (**) by two-tailed Student's t test.

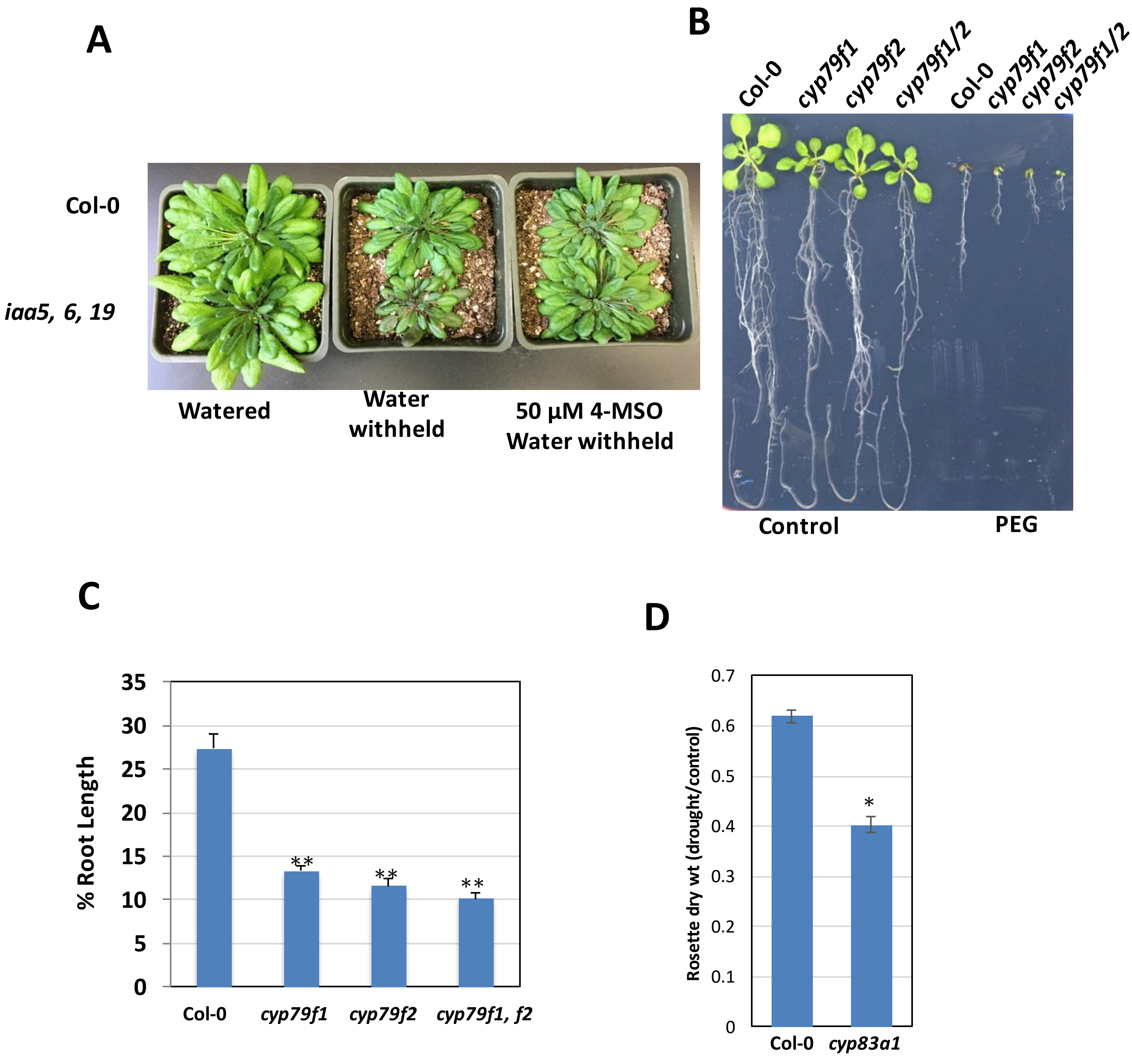

Supplementary Figure S2. Aliphatic glucosinolate biosynthetic mutants are less tolerant of drought or dehydration. (**A**) The *iaa5,6,19* triple mutant is less drought tolerant than the wild type in a water withholding experiment. **(B)** Representative 15-day-old *cyp79f1*, *cyp79f2* and *cyp79f1f2* seedlings after PEG stress. (**C**) % root length relative to growth on control medium from (B)**.** Results are presented as the mean ± SE of one experiments with n=12-15 independent seedlings. (**D**) The *cyp83a1* mutant is less drought tolerant than wild type in a water withholding experiment. For (**C**) and (**D**) differences are significant at $p < 0.05$ (*) and $p < 0.01$ (**) by two-tailed Student's t test.

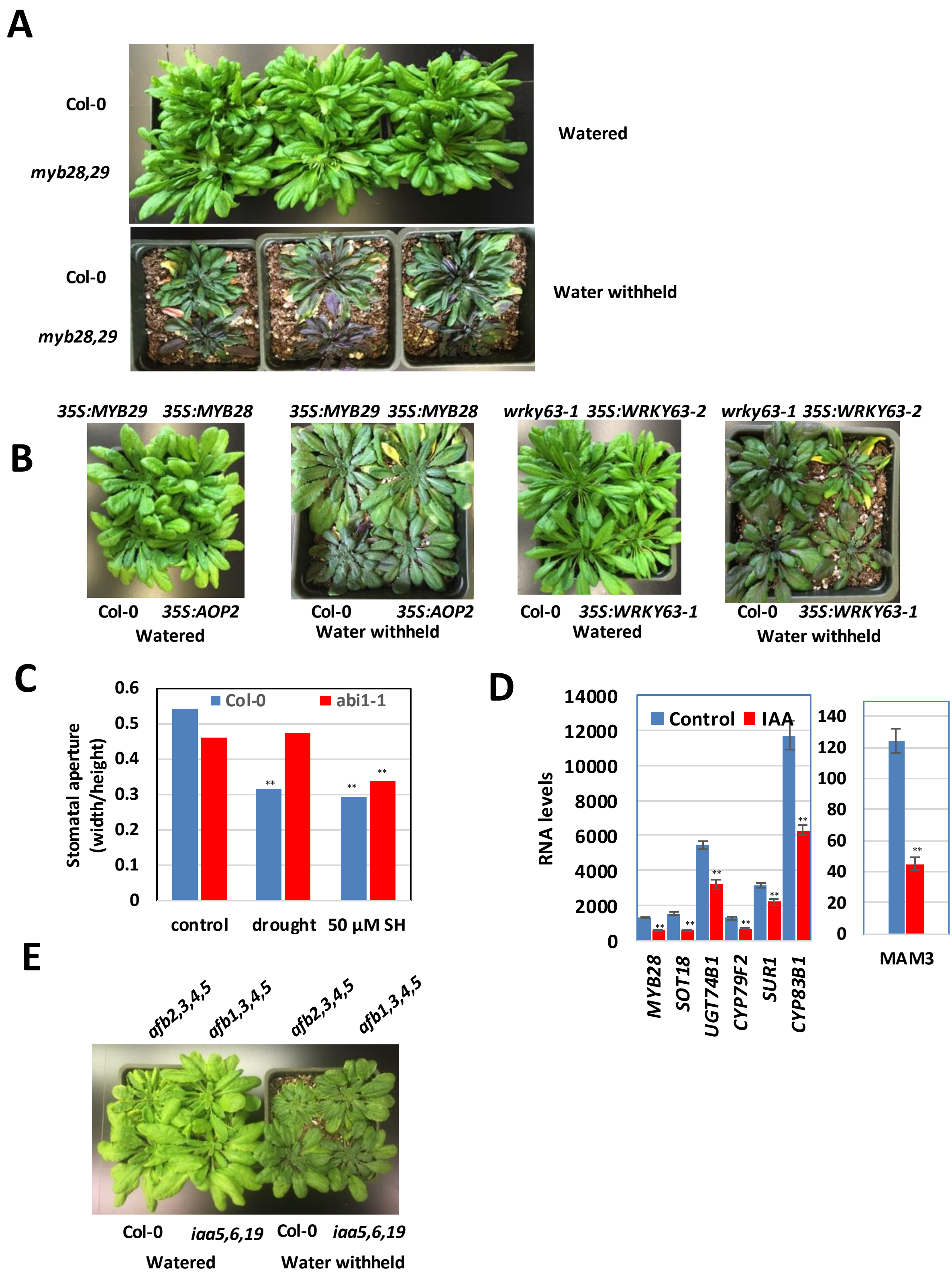
A
Col-0
myb28,29
Watered
Col-0
myb28,29
Water withheld
B
35S:MYB29 35S:MYB28
Col-0 35S:AOP2
Watered
35S:MYB29 35S:MYB28
Col-0 35S:AOP2
Water withheld
wrky63-1 35S:WRKY63-2
Col-0 35S:WRKY63-1
Watered
wrky63-1 35S:WRKY63-2
Col-0 35S:WRKY63-1
Water withheld
C
Stomatal aperture (width/height)
Col-0
abi1-1
control
drought
50 µM SH
D
RNA levels
Control
IAA
MYB28
SOT18
UGT74B1
CYP79F2
SUR1
CYP83B1
MAM3
E
afb2,3,4,5
afb1,3,4,5
afb2,3,4,5
afb1,3,4,5
Col-0
iaa5,6,19
Col-0
iaa5,6,19
Watered
Water withheld

Figure S3. Response of *MYB28, MYB29, AOP2* and *WRKY63* mutant and transgenic plants to water withholding. (**A**) The *myb28,29* double mutant is less drought tolerant than the wild type in a water withholding experiment. (**B)** Overexpression of *MYB28*, *MYB29* and *AOP2* results in increased tolerance to water withholding, while *35S:WRKY63* lines are less tolerant in this assay. (**C**) Stomatal response of Col-0 and *abi1-1* 50 µM sinigrin hydrate. (**D**) GLS biosynthetic genes are repressed by auxin treatment as shown by qPCR analysis. (**E**) *afb* higher order mutant plants are more drought tolerant than wild type in a water withholding experiment. Differences are significant at $p < 0.05$ (*) and $p < 0.01$ (**) by two-tailed Student's t test.

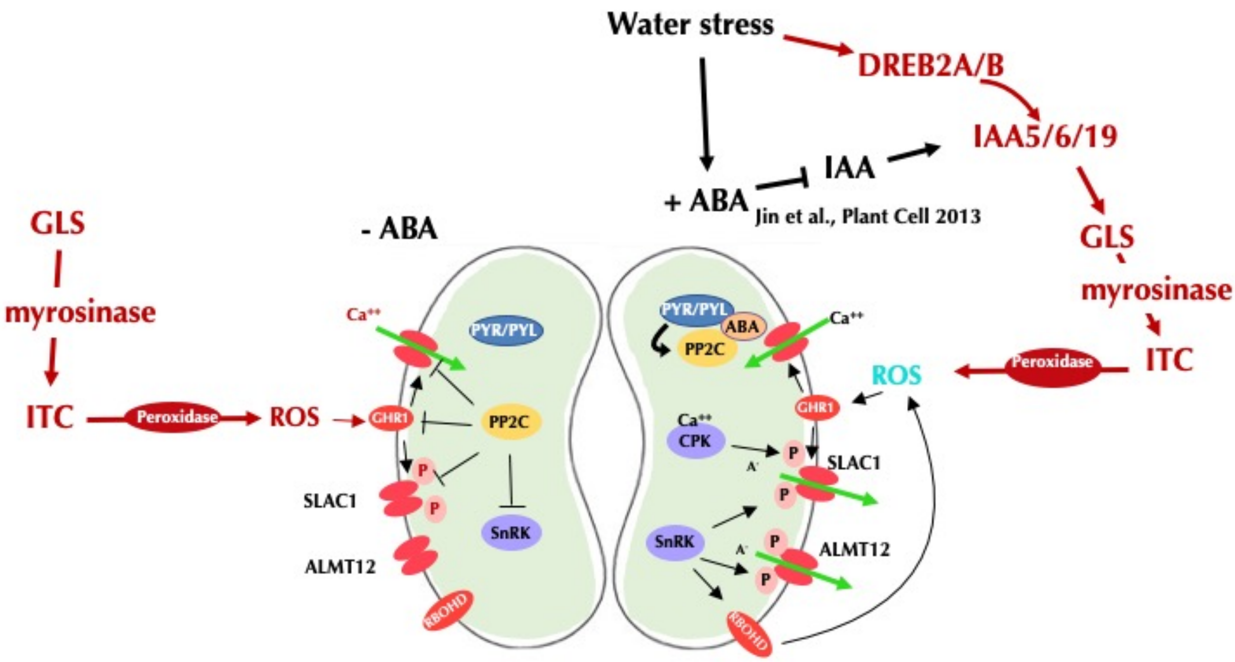

Fig S4. A proposed model for GLS action during stomatal regulation. Adapted from (43). GLS regulation diagramed in red. Water deficit induces DREB2A/B expression which promotes expression of IAA5/6/19 and maintenance of GLS levels. Myrosinase acts on GLS to produce isothiocyanate (ITC) which results in production of ROS via a peroxidase (44). An increase in ABA levels also results in decreased IAA levels in guard cells (45) which acts to stabilize IAA5/6/19. In the absence of water stress, GLS acts to promote stomatal closure via ROS production.